
CMS Paper

2010/02/16

Measurement of the Muon Stopping Power in Lead Tungstate

The CMS Collaboration^{*}

Abstract

A large sample of cosmic ray events collected by the CMS detector is exploited to measure the specific energy loss of muons in the lead tungstate (PbWO_4) of the electromagnetic calorimeter. The measurement spans a momentum range from $5 \text{ GeV}/c$ to $1 \text{ TeV}/c$. The results are consistent with the expectations over the entire range. The calorimeter energy scale, set with $120 \text{ GeV}/c$ electrons, is validated down to the sub-GeV region using energy deposits, of order 100 MeV , associated with low-momentum muons. The muon critical energy in PbWO_4 is measured to be $160^{+5}_{-6} \pm 8 \text{ GeV}$, in agreement with expectations. This is the first experimental determination of muon critical energy.

^{*}See Appendix A for the list of collaboration members

1 Introduction

The electromagnetic calorimeter (ECAL) of the Compact Muon Solenoid (CMS) experiment [1] has been designed with a stringent performance goal on energy resolution, driven by the capability to detect a Higgs boson decaying into two photons. While waiting to record events from beam collisions at the LHC, its outstanding characteristics have been exploited to measure the muon stopping power in lead tungstate (PbWO_4) for cosmic ray muon momenta between 5 and 1000 GeV/c .

The stopping power for muons in the energy range considered can be conveniently written as

$$f(E) = \left\langle -\frac{dE}{dx} \right\rangle = a(E) + b(E)E, \quad (1)$$

where E is the total muon energy, x is the thickness of the traversed material, commonly measured in mass per unit surface, $a(E)$ is the stopping power due to collisions with atomic electrons, and $b(E)$ is due to radiative processes: bremsstrahlung, direct pair production, and photonuclear interactions; $a(E)$ and $b(E)$ are slowly varying functions of E at energies where radiative contributions are important [2, 3].

Numerical values of stopping power and related quantities quoted throughout this paper are taken from tables in [4]. The tables [see 2] are obtained from calculations following [3] including post-Born corrections from [5], which result in an increase of the critical energy by 6 GeV. The theoretical uncertainties are everywhere smaller than the statistical precision of the results reported in this paper. The definition of critical energy as the energy at which the average rates of energy loss through collision and radiation are equal [2, 3] is adopted in this paper.

The lowest and highest momenta considered in the analysis reported here correspond to regions dominated by collision and radiative processes, respectively. Comparison of the experimental values of the stopping power with predictions, extends the validity of the ECAL energy scale, set with 120 GeV/c electron beams, down to energy deposits below 1 GeV. Analysis of data in the full momentum range permits a comparison of collision losses with radiative losses, thus leading to the first experimental determination of muon critical energy.

The experimental setup and the characteristics of the data sample are described in Section 2. Event selection and measurement of relevant physical quantities are discussed in Section 3. Possible limitations in the measurement of the muon stopping power are addressed in Section 4. In Section 5, corrections for systematic effects and statistical issues are addressed, and results are reported.

2 Experimental setup and data sample

The data set consists of cosmic ray muons traversing the CMS detector located 100 m underground, collected during the detector commissioning phase.

The central feature of the CMS apparatus is a superconducting solenoid of 6 m internal diameter. Within the field volume are the silicon pixel and strip tracker, the crystal electromagnetic calorimeter and the brass-scintillator hadron calorimeter (HCAL). Muons are measured in gas-ionization chambers embedded in the steel return yoke. In addition to the barrel and endcap detectors, CMS has an extensive forward calorimetry. The silicon pixel and strip detectors provide excellent momentum reconstruction, with a 10 % resolution for 1 TeV/c muons passing close to the nominal interaction vertex.

The electromagnetic calorimeter is a hermetic homogeneous scintillator detector made of PbWO₄ crystals. Lead tungstate has a high density (8.3 g cm^{-3}), a short radiation length, ($X_0 = 0.89 \text{ cm}$) and a small Moliere radius ($R_M = 2.0 \text{ cm}$). Crystals are organized in a central barrel of 61 200 crystals closed by two end-caps of 7324 crystals each. The light is read out by avalanche photodiodes (APD) in the barrel and by vacuum phototriodes (VPT) in the end-caps. In the barrel, relevant to the analysis presented in this paper, the individual crystals have a truncated-pyramid shape with a mean lateral size in the front section of 2.2 cm and a length of 23 cm, which corresponds to 25.8 radiation lengths. The barrel crystals are organized in a quasi-projective geometry, where their principal axis is tilted by 3° with respect to the nominal interaction vertex, in both the azimuthal and polar angle projections.

The CMS collaboration conducted a month-long data-taking exercise, known as the Cosmic Run At Four Tesla (CRAFT), during October-November 2008 with the goal of commissioning the experiment for extended operation [6]. With all installed detector systems participating, CMS recorded 270 million cosmic ray triggered events with the solenoid at its nominal axial field strength of 3.8 T. An event display of a cosmic ray muon crossing CMS is shown in Fig. 1.

During data taking at the LHC, the APDs will be operated at a gain of 50. In order to increase the sensitivity to low-energy deposits and to reduce the impact of the electronic noise, the APD gain was raised to 200 for several of the commissioning runs. In this condition the noise per readout channel amounts to about 1 ADC count, which corresponds on average to 9.3 MeV [7].

The signal from the APDs, after being amplified and shaped, is digitized at 40 MHz and ten pulse samples are recorded for each calorimeter channel. In order to reduce the bandwidth required for data acquisition, a reduction procedure is applied. A summary of data reduction algorithms is reported in Section 3; for more details the reader is referred to [8].

Because of the angular distribution of the cosmic ray muon flux and the lower sensitivity of the ECAL end-caps to the energy released by a minimum ionizing particle, only the barrel part of ECAL is used in the present analysis.

3 Event measurement and selection

The physical variables to be measured for each muon are the momentum, the path length in ECAL, and the energy lost in ECAL.

The muon momentum is measured from the track fit performed in the inner tracking system [9].

The path length in ECAL is estimated by propagating the measured muon track inside the calorimeter taking into account bending due to the magnetic field and expected energy loss. The average path length in ECAL for the selected muon sample is 22.0 cm, with an rms spread of 2.6 cm.

A dedicated algorithm has been developed to reconstruct the energy deposited by cosmic ray muons in ECAL. The main differences with respect to the standard reconstruction algorithm for events collected during LHC operation are driven by the requirement of good reconstruction and association efficiency down to low energy and for energy deposits associated with muons not pointing to the nominal interaction vertex. Online data reduction is based on zero suppression (ZS), that is, a readout of channels above the ZS threshold, and on a full readout of selected regions (SR) of high interest, as identified by a Selective Readout Processor (SRP), based on the information of the Level-1 trigger system of ECAL [8]. For CRAFT runs with APD gain set to 200, the ZS threshold corresponds to about 20 MeV and the SR threshold to about 170 MeV.

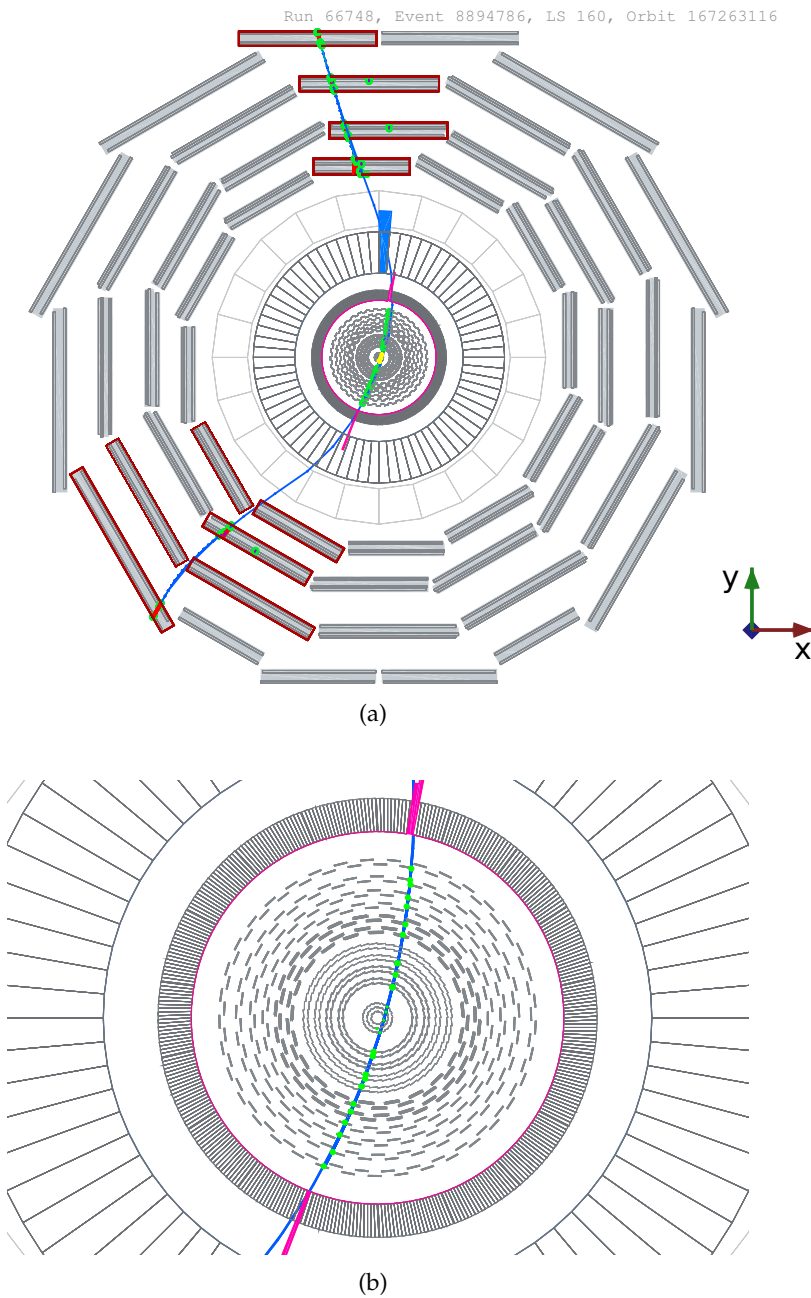


Figure 1: An event display of a cosmic ray muon crossing CMS: (a) the full detector and (b) a detail of the central region. ECAL hits are in magenta, HCAL hits in blue, tracker and muon hits in green. The views represent a section of CMS in a plane perpendicular to the beam direction, the *x* axis pointing to the centre of the LHC ring and the *y* axis pointing vertically upwards.

When the condition for SR is met, a matrix of 3×3 trigger towers is read out. Each tower is comprised of 5×5 crystals, the matrix is centered around the tower with energy deposit above the SR threshold. The energy reconstruction algorithm identifies clusters starting from a central crystal (seed) with an energy deposit of at least 15 ADC counts (139.5 MeV), or from the most energetic of a pair of adjacent crystals with at least 5 ADC counts (46.5 MeV) each, the cluster energy is determined as the sum of all channels above 2 ADC counts (18.5 MeV) belonging to a 5×5 matrix of crystals.

Contiguous clusters are merged and the size of the resulting cluster depends on the impact angle of the muon at the calorimeter surface. Clusters in ECAL are then associated with muon tracks according to a geometrical match between the track extrapolation to the calorimeter surface and the centre of gravity of the energy deposit. The energy in the cluster is obtained after application of relative calibration constants to individual channels and of an absolute energy scale factor. The intercalibration constants are defined to equalize the response of the individual channels to the same energy deposits in the corresponding crystals. The absolute energy scale was determined from data taken with a 120 GeV/c electron beam [10]. It is defined as the response to 120 GeV/c electrons striking the centre of a 5×5 matrix of crystals in a reference region of ECAL. With these definitions, the same energy scale is obtained over the entire ECAL up to local containment effects. According to Monte Carlo simulation, this containment factor corresponds to 97 % of the electron energy for an impact at the point of maximum response of the reference crystal matrix. Energy deposits due to non-radiating relativistic particles are fully contained in a 5×5 crystal matrix, thus the energy scale defined at the test beam is scaled by 0.97 to measure the ECAL response to muons. Additional corrections, related to containment effects due to leakage from the crystals of muon induced secondary particles, are addressed in Section 5.

Only runs in which the APD gain was set to 200 are considered in the present analysis. The useful sample of CMS triggers is thus reduced to 8.8×10^7 . Furthermore, muons are required to cross both the upper and the lower half of ECAL barrel (see Section 5). The initial sample of events considered in the present analysis was thus defined by the combined requirements of a muon at the trigger level [11], of a single muon track reconstructed by the tracker [9], and of an energy deposit associated with the track in both the upper and the lower half of ECAL barrel. Moreover, analysis is limited to muons with momentum ranging from 5 to 1000 GeV/c. This interval, which is mainly determined by the size of the event sample, is further divided for analysis purposes into 20 equal bins in $\log(p)$. For the present analysis, the muon momentum has to be measured upstream of the energy release in the calorimeter. Thus only energy deposits in the bottom half of ECAL are used. The following selections are then applied to the initial sample: the uncertainty on muon momentum must be smaller than the bin width; the ratio of the energy deposit in the calorimeter to muon momentum must be less than 1 within the experimental accuracy; the angle between the muon track at the ECAL surface and the corresponding crystal axis must be smaller than 0.5 radians. These criteria reduce the sample by a factor 1.7, the largest reduction coming from the angle selection. Moreover, as will be clarified in Section 5, events with energy deposits above 500 MeV in the upper part of the ECAL barrel are vetoed. This last selection further reduces the sample by a factor 1.15. The final sample consists of 2.5×10^5 muons.

The measured muon spectrum, after the selections, is shown in Fig. 2(a). The spectrum of energy deposited in crystals is shown in Fig. 2(b).

Figure 3 displays the distributions of $\Delta E / \Delta x$, the measured cluster energy divided by the path length in ECAL, for muons with momentum below 10 GeV/c, where collision losses domi-

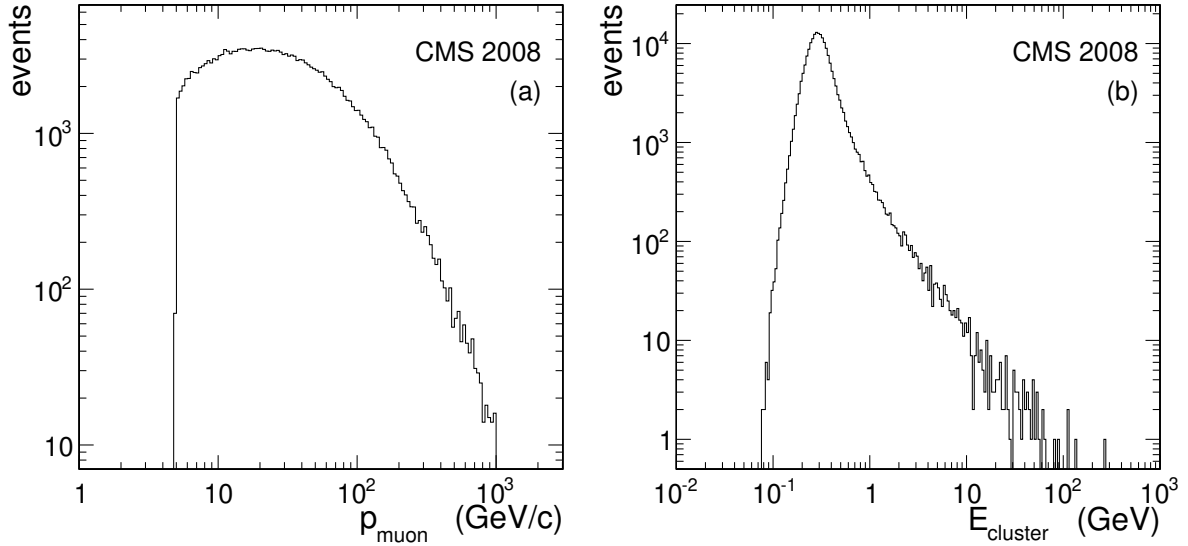


Figure 2: (a) Momentum spectrum of the muons passing the selections; (b) spectrum of the reconstructed energy in the lower ECAL hemisphere. A logarithmic binning is used.

nate (a), and for muons with momentum above 300 GeV/ c , where sizable radiation losses are expected (b).

4 Measurement of the stopping power

In making a calorimetric measurement of stopping power, the choice of optimal thickness of the sampling material must be the result of a compromise. On the one hand, the thickness should be small enough for the variation of primary particle energy to be negligible; on the other, the thickness should be large enough to allow a precise measurement of the energy released. Furthermore, the correction arising from energy leaking from the measurement volume should be kept small. The extent to which the CMS ECAL crystals meet these requirements is discussed in 4.1 and 4.2.

4.1 dE/dx approximation

The stopping power is experimentally determined by the measurement of the energy ΔE lost by a muon when traversing a known thickness Δx , which must be small in order that the approximation $f(E) = -dE/dx = \Delta E/\Delta x$ holds. Quantitatively $\Delta f/f$, where $\Delta f = f(E) - f(E - \Delta E)$, has to be smaller than the desired relative precision on the measurement of f . Since

$$\Delta f \sim \frac{df}{dE} \frac{dE}{dx} \Delta x \quad (2)$$

then

$$\frac{\Delta f}{f} \sim \frac{df}{dE} \Delta x. \quad (3)$$

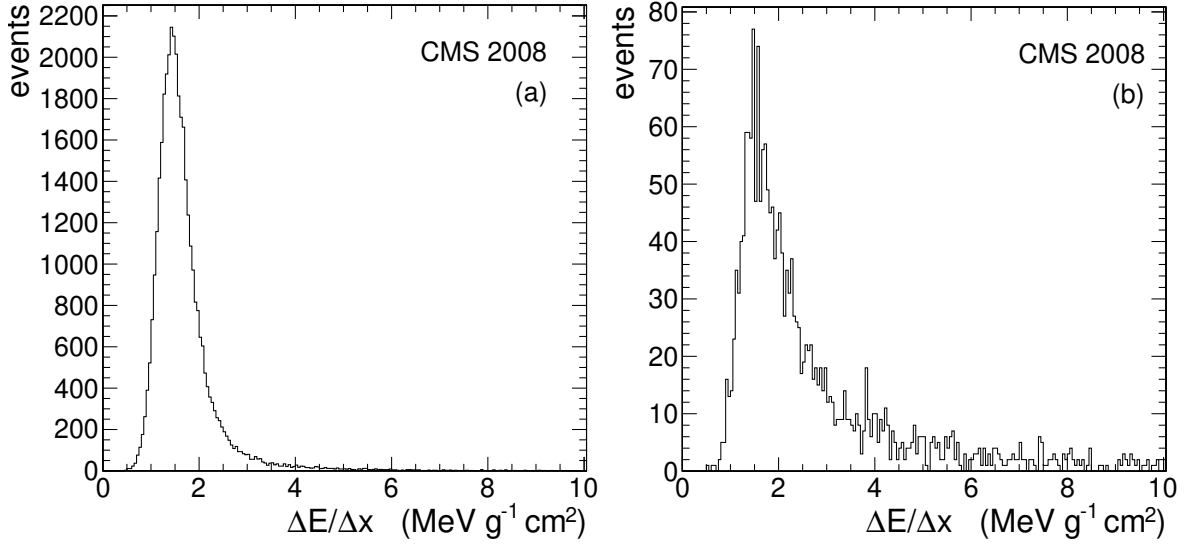


Figure 3: Measured distributions of $\Delta E/\Delta x$ in ECAL; (a) for muon momenta below $10 \text{ GeV}/c$; (b) for muon momenta above $300 \text{ GeV}/c$; the fraction of events with $\Delta E/\Delta x > 10 \text{ MeV g}^{-1} \text{ cm}^2$ is 1.3×10^{-3} and 8×10^{-2} in (a) and (b) respectively.

In the present case, Δx is typically 180 g/cm^2 (about $25 X_0$ in PbWO_4). The derivative of the stopping power with respect to E can be written as a sum of the contributions of collision and radiation processes, namely

$$\frac{\Delta f}{f} = \left[\left(\frac{df}{dE} \right)_{coll} + \left(\frac{df}{dE} \right)_{rad} \right] \Delta x. \quad (4)$$

For the scope of this analysis, $b(E)$ in Eq. 1 can be assumed to be constant, with a value equal to that at 1 TeV . Then $(df/dE)_{rad} = b = 1.4 \times 10^{-5} \text{ cm}^2/\text{g}$ [4].

This corresponds to a muon radiating $1/400$ of the energy when traversing $\Delta x = 180 \text{ g/cm}^2$. Its average contribution to $\Delta f/f$ is then $1/400$, which is negligible when compared to the precision of the measurement.

The component of the derivative due to collisions is a monotonically decreasing function of E in the energy range of the present measurement; its expected value at the lowest momentum ($5 \text{ GeV}/c$) is $2.6 \times 10^{-5} \text{ cm}^2/\text{g}$ [4]. Thus $\Delta f/f$ is everywhere small when compared with other sources of uncertainty.

The above arguments apply not only to muons losing an energy equal to the expectation value, but also to the case of large fluctuations occurring in radiative processes. In fact $f(E)$ is essentially a linear function of E in this energy range.

4.2 Containment effects

Energy lost by a muon is transferred to energy of secondaries. Since secondaries and their daughters may travel a significant distance, the energy lost by a muon traversing a given volume is in general different from the energy deposited in that same volume. The energy ΔE considered in the previous section is the energy lost by a muon along a given path, while the

first output of the measurement procedure is the energy deposited in a given volume of the calorimeter. Taking as a reference volume a cylinder with its axis along the muon direction, energy flow across the lateral surface can be made negligible by choosing a sufficiently large radius. On the other hand there is always a non-negligible flow of energy carried by secondaries entering and leaving the two ends of the cylinder, since secondaries are produced along the entire muon path. In a homogeneous material an equilibrium between the energy flowing in through the front surface and the energy flowing out of the rear surface is approximately reached when the front surface is preceded by at least an amount of material corresponding to the energy-weighted average range of secondaries. In fact, considering a muon entering a dense homogeneous material from vacuum, the average energy deposition per unit thickness is given by the convolution product of a step function equal to the muon stopping power (muon passing from vacuum to homogeneous material) with the function $S(t)$ describing the average fractional energy deposition density as a function of depth t for secondaries (i.e. the shower depth-profile for high-energy electrons and photons). This convolution product at depth x in the material is equal to the muon stopping power times the definite integral from 0 to x of $S(t)$. Considering, as an illustration, the non-physical case of a muon whose only interaction with matter is photon radiation, at a depth in the dense material at which an electromagnetic shower would have deposited 90 % of its energy, the ratio between the average energy deposition density and the stopping power would be 0.9. Therefore, considering the spectra of secondaries produced by muons, it is found that the equilibrium condition is approached for δ -electrons after the muon has traversed a thickness of about 10 g/cm^2 , while for radiated photons it is approached after about 20 radiation lengths.

In the present case, the situation is well described as a homogeneous region of PbWO_4 preceded by order of 10 g/cm^2 of nearby material. Because of the presence of a strong magnetic field, material separated by more than a few tens of centimeters from the crystals is less effective in producing secondaries flowing into the measurement volume. Thus the crystals diametrically opposite to those under study (corresponding to a separation of approximately 2.6 m) have little effect on the measured energy loss. Therefore, net containment corrections are expected to be small or negligible for collision losses, but sizable for radiative losses. A quantitative estimate of these corrections has been obtained by means of a dedicated simulation based on the Geant4 package [12], as detailed in Section 5.

5 Data analysis and experimental results

This section first addresses corrections to systematic effects; instrumental effects are considered in 5.1; the physics effects identified in Section 4 are considered in 5.2. Statistical analysis of data and experimental results are then discussed in 5.3.

5.1 Instrumental effects

The relevant instrumental effects are related to the online data reduction and to the energy reconstruction procedure described in Section 3.

The presence of thresholds introduces a bias in energy reconstruction: noise fluctuations above threshold contribute a positive bias, while energy deposits below threshold contribute a negative bias.

When the muon direction is close to the crystal axis, the energy deposited in ECAL is in most cases above the SR threshold (90 % of events with the angle between muon and crystal axis smaller than 0.1 radians). When this condition is met, the bias arises mainly from effects asso-

ciated with the clustering threshold and the noise spectrum, signals below threshold making a negligible contribution. The probability of noise fluctuation above threshold is measured in a dedicated analysis of the noise spectrum. A 14.7 MeV bias is estimated for muons at angles smaller than 0.1 radians. At larger muon angles to the crystal axis, the average energy deposit per crystal decreases. Therefore conditions for ZS read-out occur more frequently, with the higher ZS threshold reducing the noise bias. Moreover, the probability that the energy deposited in a single crystal is below clustering threshold increases, thus contributing a negative bias. Bias is then expected to decrease with increasing angles, but its estimate depends on several contributions, and is less reliable than the estimate at small angles. Both a Monte Carlo simulation and the analysis of crystal multiplicity versus angle in experimental data indicate a constant positive bias (plateau) at small angles, followed by a monotonic decrease at larger angles.

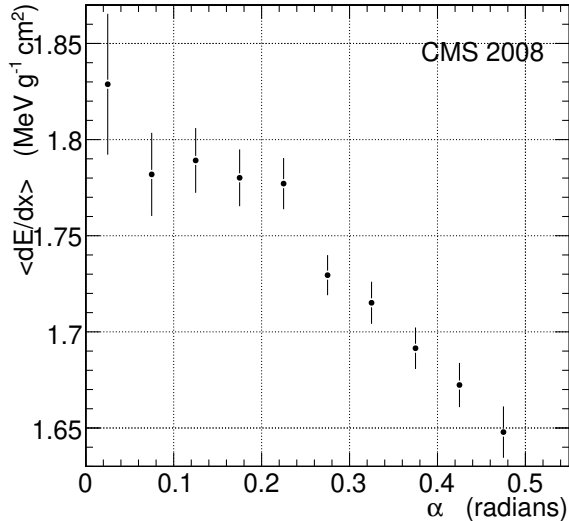


Figure 4: Dependence of the raw $\langle dE/dx \rangle$ on the angle α between the muon direction and the crystal axis, for muon momentum between 5 and 10 GeV/c. Vertical bars represent statistical errors.

Bias dependence on angle for non-radiating muons has been further studied by analyzing the dependence of the raw dE/dx on angle for muons below 10 GeV/c in experimental data. The result, shown in Fig. 4, is consistent with expectations, although it is not inconsistent with a wider plateau, extending up to 0.2 radians, or with a linear dependence of bias on angle with no plateau. A bias correction, dependent on angle, is thus applied to the estimated collision component of the stopping power, by applying the following procedure. At small angles, the bias to be subtracted is 14.7 MeV. At larger angles, the bias to be subtracted is estimated from a fit to the data shown in Fig. 4, assuming a plateau followed by a linear decrease with angle. The central value of the bias estimate is obtained assuming that the plateau extends up to 0.1 radians, the hypotheses of no plateau and of a plateau up to 0.2 radians are taken as extreme cases in the evaluation of the systematic uncertainty of bias subtraction. The uncertainty in the evaluation of the 14.7 MeV bias and the statistical uncertainty of the fit also contribute to the systematic uncertainty of the bias correction. The overall systematic uncertainty is estimated to be 3.5 MeV, which corresponds to about 1.2 % of the average energy deposited by a low-momentum muon.

The bias is estimated to be negligible in the presence of the larger energy deposits associated

with radiative processes; it is in any case negligibly small compared to the systematic effects discussed in Section 5.2. Therefore, no bias correction is applied to the expected contribution to dE/dx from radiative processes over the entire muon momentum spectrum.

5.2 Containment corrections

Energy leakage and the effects of upstream and downstream materials are quantitatively different for collisions and radiative processes. Therefore, in order to make an experimental determination of the muon critical energy, losses and compensation for radiative and collision processes are treated separately.

To estimate the difference between energy lost and energy deposited in ECAL, a model based on the Geant4 simulation toolkit, with a simplified description of the detector and materials surrounding it, was developed. The use of a simplified simulation instead of the full simulation available in CMS was driven by the high statistics needed for these studies and for those reported in Section 5.3. The results of the simulations were also compared with dedicated analytical calculations.

Because of the effect of the intense magnetic field on the trajectories of charged particles, material lying more than a few tens of centimeters away from the crystals under study may be neglected. In particular, the upper half of the ECAL has been ignored in the simulation. The validity of this approximation has been reinforced by selecting muons that produce a signal of less than 500 MeV in the upper part of the ECAL, thus removing most of those emitting a hard photon. As a further check, the energy deposited in the lower half of ECAL by muons releasing less than 500 MeV in the upper ECAL hemisphere (the selected sample) has been compared with the complementary sample and agreement was found within the precision of the comparison. In fact, in the muon momentum region between 145 and 1000 GeV/c , where radiative losses are relevant, the weighted average of the ratio of the dE/dx measured in the two samples in seven momentum bins is 0.95 ± 0.09 . This result gives no indication of an effect of the upper part of ECAL on the energy deposited in the lower part, thus supporting the hypothesis that far material can be neglected. However, due to the modest statistical precision of this test, it was conservatively decided to activate the veto in the event selection.

The low-momentum region is of major interest for the present analysis, since the large sample size and the small energy loss fluctuations allow precise results to be obtained. According to the simulation, the energy carried by secondaries flowing out of the rear detector surface is, on average, 3 % of the energy lost in the crystals for a muon with momentum 15 GeV/c . This represents an upper limit to containment corrections in the low-momentum region, where collision losses dominate. In fact, as already discussed in Sect. 4.2, the rear leakage can be compensated by secondaries produced in upstream material entering the front detector surface. A comparison of the deposits in the upper and lower hemispheres of the ECAL barrel, for muons with momentum between 5 and 10 GeV/c , shows no difference in dE/dx , with a sensitivity better than 1 % [7]. Given the similarity of the results, in spite of the asymmetric distribution of the outer and inner material around ECAL, the net correction has been neglected, and 1 % systematic uncertainty on the null correction for collision losses has been assumed.

Estimated corrections for energy containment in radiative processes have been derived from dedicated simulations of two extreme cases: with no material in front of ECAL and with the whole material budget of the tracker concentrated just in front of ECAL. The former case represents the upper limit to the containment correction, where only rear losses are considered; the latter case gives a lower limit to the correction, as it maximally overestimates the energy flow through the front face due to upstream material. In both cases the effects of the upper

ECAL hemisphere, used as a veto in the analysis, were ignored. The mean value and half of the difference between the results of the two simulations are the estimate of the corrections for the energy containment in radiative processes and of the associated systematic error. The correction for energy leakage in radiative processes is maximal at $1 \text{ TeV}/c$: at this muon momentum it corresponds to $(28 \pm 5)\%$ of the average energy lost, while at $170 \text{ GeV}/c$ it reduces to $(14.5 \pm 2.5)\%$, where the error arises from the systematic uncertainty mentioned above. The uncertainty is small compared to the statistical uncertainty in the measurement of the stopping power in the corresponding region. Given the size of statistical uncertainty and the contribution from other sources of systematic errors, the precision of the correction obtained with the simplified simulation is sufficient over the entire momentum range. The correction for non-containment of radiated secondaries is applied over the whole momentum spectrum to the expected contribution of radiative processes to stopping power.

5.3 Critical energy, energy scale, Cherenkov contribution

Several possible sources of systematic error have been taken into account in making a comparison between the energy scale of the ECAL set with a $120 \text{ GeV}/c$ electron beam and the scale resulting from the measurement of muon stopping power.

Four out of 36 supermodules were calibrated with $120 \text{ GeV}/c$ electrons. The energy scale was transferred to all supermodules by means of the cosmic ray intercalibration discussed in [10]. This procedure resulted in a typical single-channel uncertainty of 1.5%, which is dominated by statistics, and an overall scale uncertainty whose contribution to the final precision of the present measurement is negligible.

The precise variation in the gain of each APD, when going from a nominal gain of 50 to a nominal gain of 200, has been measured by means of the laser monitoring system described in [1]. The resulting uncertainty on the average energy scale is negligible.

The overall variation of the response to incident electrons with temperature has been measured in test beam to be $-(3.8 \pm 0.4)\% \text{ }^{\circ}\text{C}^{-1}$. In CMS, the temperature is monitored with a $0.01\text{ }^{\circ}\text{C}$ precision, and the cooling system has been demonstrated to maintain the temperature stable to $18 \pm 0.1\text{ }^{\circ}\text{C}$ [1, 7], thus uncertainties on temperature corrections are negligible.

A test of reproducibility of calibration constants was performed by exposing the same module to test-beam electrons on two occasions, separated by 30 days. This resulted in no measurable offset on the energy scale [10].

A different pulse height reconstruction procedure is required for cosmic-ray data, which are asynchronous with respect to detector clock, compared to collision data, which are synchronous, or to test-beam data, which are also asynchronous but were recorded together with accurate timing information from trigger. This has been estimated to introduce a systematic uncertainty of 1% in the energy scale of cosmic ray data with respect to test beam.

In Fig. 5(a), the specific muon energy loss resulting after corrections is compared to expectations as a function of the muon momentum [4]. Fig. 5(b) shows the ratio of experimental measurements to expected values. Two regions are indicated in Fig. 5: the expected 68 % probability central interval (grey shaded area), and the minimum interval corresponding to 68 % probability (region delimited by continuous curves). The reasons for considering both intervals and the procedure adopted for their estimate are summarized below.

The characteristics of radiative losses, which correspond to rare processes with high energy releases, generate probability distribution functions (pdf) of energy loss for single events with

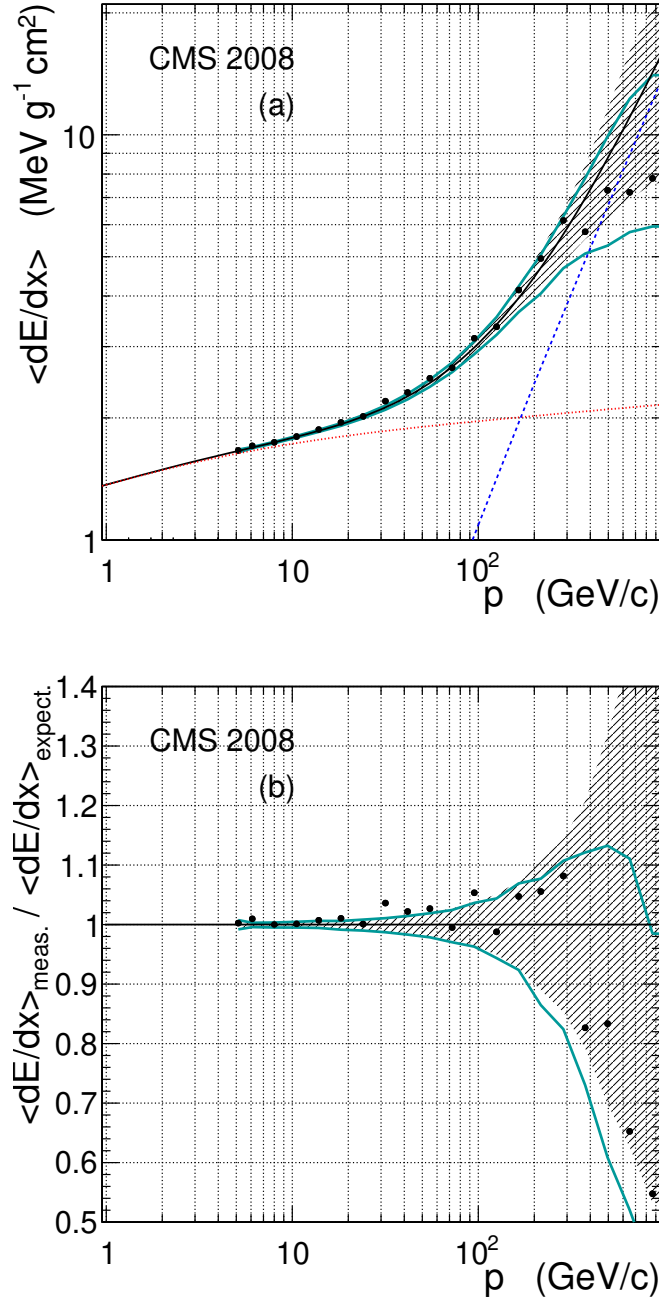


Figure 5: (a) Muon stopping power measured in PbWO₄ (dots) as a function of muon momentum compared to expectations [4] (continuous black line). The expected contributions from collision and radiative processes are plotted as well (red dotted line and blue dashed line respectively). (b) Ratio of the measured and the expected values of the muon stopping power, as a function of muon momentum. As discussed in the text, in both figures, the shaded grey area indicates the expected 68 % probability central interval, while the continuous cyan curves delimit the minimum interval containing 68 % of the expected results. “Experimental errors” are not shown for reasons discussed in the text.

long tails at high energy, that is: highly positively skewed distributions. In this condition, convergence to a normal distribution for the average dE/dx of a sample of N events is slow. The skewness of the single event distribution increases with increasing muon momentum, owing to the increasing contribution of radiative losses with momentum. The number of events per bin in the selected data sample rapidly decreases with momentum for $p > 50 \text{ GeV}/c$ (Fig. 2(a)). It is thus expected that, due to the combined effect of increasing skewness of single event distribution and decreasing event statistics with increasing momentum, in the higher momentum bins the pdf of the sample mean of dE/dx cannot be approximated by a Gaussian. Moreover, when this condition occurs, sample mean and sample variance are highly correlated. It follows that the widely used “experimental error”, namely the sample rms divided by the square root of the sample population, is not a good measure for the consistency of the sample mean with the expected value. Therefore the uncertainty of the result has been estimated, consistently over the entire momentum range covered by the measurement, by means of a numerical technique based on the simulation of the expected results with Geant4. Ten thousand identical experiments, each with the same statistics per momentum bin as the actual data sample, were simulated. The expected pdf of the mean is then obtained for each bin as the distribution of the mean values of the stopping power from the different experiments. For each pdf two 68 % probability intervals for the expected result were derived: the central interval, obtained by discarding 16 % of the results on each tail of the pdf, and the interval of minimum width containing 68 % of the results; this last interval always contains the most probable value. For Gaussian distributions these intervals coincide. In Fig. 5, for the event samples corresponding to the bins above $100 \text{ GeV}/c$, the differences between the two intervals become increasingly significant. At lower momenta, where the two intervals tend to coincide, they also correspond to the conventional estimate of the experimental error.

For the high momentum bins, the increasing probability of large fluctuations in radiative energy losses, combined with the decreasing size of the event samples, cause the most probable values to be systematically lower than the expectation values. This trend is particularly marked in the highest momentum bin of Fig. 5, where the expectation value lies outside the 68% probability interval.

The curve

$$(dE/dx)_{\text{meas}} = \alpha \left[\left(\frac{dE}{dx} \right)_{\text{coll}} + \beta \times \left(\frac{dE}{dx} \right)_{\text{rad}} \right],$$

where *coll* and *rad* label the predicted energy losses in PbWO₄ due to collisions with atomic electrons and radiative processes respectively [4], is fitted to experimental stopping power data using a binned maximum likelihood and the pdf described above. The parameters α and β account for the overall normalization of the energy scale and for the relative normalization of radiation and collision losses. With the adopted parameterization the β parameter, from which the critical energy is measured, is independent of the overall energy scale. The fit results in:

$$\begin{aligned} \alpha &= 1.004^{+0.002}_{-0.003} \text{ (stat.)} \pm 0.019 \text{ (syst.)} \\ \beta &= 1.07^{+0.05}_{-0.04} \text{ (stat.)} \pm 0.6 \text{ (syst.)}. \end{aligned}$$

Adding statistical and systematic contributions in quadrature, it may be concluded from the above results that the energy scale is consistent with expectations within a systematic uncertainty of 1.6 %, with a 1.2 % contribution from the uncertainty on the energy scale dependence

on the angle and on the clustering, and a 1.0% contribution from uncertainty in containment corrections. This result is mainly determined by the precision of the measurements in the momentum region below $20 \text{ GeV}/c$, where radiation losses are marginal. The typical energy released in this region is about 300 MeV. Thus the energy scale set with $120 \text{ GeV}/c$ electrons still holds in the sub-GeV region. This, assuming a linear response of the detector to the collected light, implies that the relative contribution to collected photons of Cherenkov light and scintillation are the same for $120 \text{ GeV}/c$ electrons and for muons in the $5\text{-}20 \text{ GeV}/c$ region, within the 1.6% precision of this measurement (this last statement strictly holds only for muons at small angle with respect to the crystal axis).

From the fit results, a muon critical energy of 160^{+5}_{-6} (stat.) ± 8 (syst.) GeV is obtained, in agreement with the computed value of 169.5 GeV for PbWO_4 [4]. The systematic uncertainty includes a contribution of 4.5 GeV from the uncertainty of the containment corrections, dominated by the limited knowledge of the correction for radiation losses, and a contribution of 6 GeV due to the stability of the result against bias subtraction and event selection. For the latter, sizable contributions come from the variation of the acceptance of the muon angle with respect to the crystal axis, and, to a lesser extent, from the requirement that E/p be lower than 1. The contributions from these sources were estimated by varying the muon acceptance angle between 0.3 and 0.7 radians, and by removing the requirement that E/p be lower than 1.

It might be argued that the use of pdf, calculated a priori in anticipation of a particular outcome, would be inappropriate when the fitted parameters differ from the expected values. In order to investigate the possible importance of this, fits were performed with alternative pdf sets, parametrized as functions of α and β , with α controlling the pdf energy scale, and β controlling the relative contributions of radiation and collisions. The changes in the results were found to be negligible compared to the quoted error.

6 Conclusions

The muon stopping power in PbWO_4 has been measured over the momentum range from $5 \text{ GeV}/c$ to $1000 \text{ GeV}/c$, yielding the first experimental determination of the muon critical energy. The value obtained: 160^{+5}_{-6} (stat.) ± 8.0 (syst.) GeV, agrees with the value calculated for this material.

In the region corresponding to muon momenta less than $20 \text{ GeV}/c$, where collision losses dominate, the average energy deposited in the crystals is of order 300 MeV. Thus the agreement (to within 1-2 %) between the measured stopping power and the calculated values confirms that the energy calibration of the detector, previously determined with $120 \text{ GeV}/c$ electrons, remains valid down to the sub-GeV scale. Alternatively, the observed linearity in energy response may be interpreted as demonstrating that the relative contributions of Cherenkov and scintillation light to the measured signal are the same for muons of $\sim 10 \text{ GeV}/c$ as for electrons of $120 \text{ GeV}/c$ (in the specific case of muons traversing the crystals at small angles with respect to the axis, and of electrons striking the crystals at normal incidence). The confirmation of the detector energy calibration and linearity of response relies on the validity of the calculated stopping power in lead tungstate, in the region dominated by collision losses. On the other hand, the value extracted for the critical energy does not depend on the energy calibration, although it would be sensitive to a deviation from linearity of the response.

Acknowledgements

We thank the technical and administrative staff at CERN and other CMS Institutes, and acknowledge support from: FMSR (Austria); FNRS and FWO (Belgium); CNPq, CAPES, FAPERJ, and FAPESP (Brazil); MES (Bulgaria); CERN; CAS, MoST, and NSFC (China); COLCIENCIAS (Colombia); MSES (Croatia); RPF (Cyprus); Academy of Sciences and NICPB (Estonia); Academy of Finland, ME, and HIP (Finland); CEA and CNRS/IN2P3 (France); BMBF, DFG, and HGF (Germany); GSRT (Greece); OTKA and NKTH (Hungary); DAE and DST (India); IPM (Iran); SFI (Ireland); INFN (Italy); NRF (Korea); LAS (Lithuania); CINVESTAV, CONACYT, SEP, and UASLP-FAI (Mexico); PAEC (Pakistan); SCSR (Poland); FCT (Portugal); JINR (Armenia, Belarus, Georgia, Ukraine, Uzbekistan); MST and MAE (Russia); MSTDS (Serbia); MICINN and CPAN (Spain); Swiss Funding Agencies (Switzerland); NSC (Taipei); TUBITAK and TAEK (Turkey); STFC (United Kingdom); DOE and NSF (USA). Individuals have received support from the Marie-Curie IEF program (European Union); the Leventis Foundation; the A. P. Sloan Foundation; and the Alexander von Humboldt Foundation.

References

- [1] CMS Collaboration, “The CMS experiment at the CERN LHC”, *JINST* **0803** (2008) S08004. doi:10.1088/1748-0221/3/08/S08004.
- [2] Particle Data Group Collaboration, C. Amsler et al., “Review of particle physics”, *Phys. Lett.* **B667** (2008) 1. doi:10.1016/j.physletb.2008.07.018.
- [3] D. E. Groom, N. V. Mokhov, and S. I. Striganov, “Muon stopping power and range tables 10-MeV to 100-TeV”, *Atom. Data Nucl. Data Tabl.* **78** (2001) 183–356. doi:10.1006/adnd.2001.0861.
- [4] Particle Data Group, “Atomic and Nuclear Properties of Materials”, *web pages at:* <http://pdg.lbl.gov/2009/AtomicNuclearProperties/> (2009).
- [5] D. Ivanov, E. A. Kuraev, A. Schiller et al., “Production of e+ e- pairs to all orders in Z alpha for collisions of high-energy muons with heavy nuclei”, *Phys. Lett.* **B442** (1998) 453–458, arXiv:hep-ph/9807311. doi:10.1016/S0370-2693(98)01278-7.
- [6] CMS Collaboration, “The CMS CRAFT Exercise”, *submitted to JINST* (2009).
- [7] CMS Collaboration, “Performance and Operation of the CMS Crystal Electromagnetic Calorimeter”, *submitted to JINST* (2009).
- [8] N. Almeida et al., “Data filtering in the readout of the CMS electromagnetic calorimeter”, *JINST* **3** (2008) P02011. doi:10.1088/1748-0221/3/02/P02011.
- [9] CMS Collaboration, “Studies of CMS Muon Reconstruction Performance with Cosmic Rays”, *submitted to JINST* (2009).
- [10] P. Adzic et al., “Intercalibration of the barrel electromagnetic calorimeter of the CMS experiment at start-up”, *JINST* **3** (2008) P10007. doi:10.1088/1748-0221/3/10/P10007.
- [11] CMS Collaboration, “Commissioning of the CMS High-Level Trigger with Cosmic Rays”, *submitted to JINST* (2009).
- [12] GEANT4 Collaboration, S. Agostinelli et al., “GEANT4: A simulation toolkit”, *Nucl. Instrum. Meth.* **A506** (2003) 250–303. doi:10.1016/S0168-9002(03)01368-8.

A The CMS Collaboration

Yerevan Physics Institute, Yerevan, Armenia
 S. Chatrchyan, V. Khachatryan, A.M. Sirunyan

Institut für Hochenergiephysik der OeAW, Wien, Austria

W. Adam, B. Arnold, H. Bergauer, T. Bergauer, M. Dragicevic, M. Eichberger, J. Erö, M. Friedl, R. Frühwirth, V.M. Ghete, J. Hammer¹, S. Hänsel, M. Hoch, N. Hörmann, J. Hrubec, M. Jeitler, G. Kasieczka, K. Kastner, M. Krammer, D. Liko, I. Magrans de Abril, I. Mikulec, F. Mittermayr, B. Neuherz, M. Oberegger, M. Padrta, M. Pernicka, H. Rohringer, S. Schmid, R. Schöfbeck, T. Schreiner, R. Stark, H. Steininger, J. Strauss, A. Taurok, F. Teischinger, T. Themel, D. Uhl, P. Wagner, W. Waltenberger, G. Walzel, E. Widl, C.-E. Wulz

National Centre for Particle and High Energy Physics, Minsk, Belarus

V. Chekhovsky, O. Dvornikov, I. Emelianchik, A. Litomin, V. Makarenko, I. Marfin, V. Mossolov, N. Shumeiko, A. Solin, R. Stefanovitch, J. Suarez Gonzalez, A. Tikhonov

Research Institute for Nuclear Problems, Minsk, Belarus

A. Fedorov, A. Karneyeu, M. Korzhik, V. Panov, R. Zuyeuski

Research Institute of Applied Physical Problems, Minsk, Belarus

P. Kuchinsky

Universiteit Antwerpen, Antwerpen, Belgium

W. Beaumont, L. Benucci, M. Cardaci, E.A. De Wolf, E. Delmeire, D. Druzhkin, M. Hashemi, X. Janssen, T. Maes, L. Mucibello, S. Ochesanu, R. Rougny, M. Selvaggi, H. Van Haevermaet, P. Van Mechelen, N. Van Remortel

Vrije Universiteit Brussel, Brussel, Belgium

V. Adler, S. Beauceron, S. Blyweert, J. D'Hondt, S. De Weirdt, O. Devroede, J. Heyninck, A. Kalogeropoulos, J. Maes, M. Maes, M.U. Mozer, S. Tavernier, W. Van Doninck¹, P. Van Mulders, I. Villella

Université Libre de Bruxelles, Bruxelles, Belgium

O. Bouhali, E.C. Chabert, O. Charaf, B. Clerbaux, G. De Lentdecker, V. Dero, S. Elgammal, A.P.R. Gay, G.H. Hammad, P.E. Marage, S. Rugovac, C. Vander Velde, P. Vanlaer, J. Wickens

Ghent University, Ghent, Belgium

M. Grunewald, B. Klein, A. Marinov, D. Ryckbosch, F. Thyssen, M. Tytgat, L. Vanelderen, P. Verwilligen

Université Catholique de Louvain, Louvain-la-Neuve, Belgium

S. Basegmez, G. Bruno, J. Caudron, C. Delaere, P. Demin, D. Favart, A. Giannanco, G. Grégoire, V. Lemaitre, O. Militaru, S. Ovyn, K. Piotrkowski¹, L. Quertenmont, N. Schul

Université de Mons, Mons, Belgium

N. Beliy, E. Daubie

Centro Brasileiro de Pesquisas Fisicas, Rio de Janeiro, Brazil

G.A. Alves, M.E. Pol, M.H.G. Souza

Universidade do Estado do Rio de Janeiro, Rio de Janeiro, Brazil

W. Carvalho, D. De Jesus Damiao, C. De Oliveira Martins, S. Fonseca De Souza, L. Mundim, V. Oguri, A. Santoro, S.M. Silva Do Amaral, A. Sznajder

Instituto de Fisica Teorica, Universidade Estadual Paulista, Sao Paulo, Brazil

T.R. Fernandez Perez Tomei, M.A. Ferreira Dias, E. M. Gregores², S.F. Novaes

Institute for Nuclear Research and Nuclear Energy, Sofia, Bulgaria

K. Abadjiev¹, T. Anguelov, J. Damgov, N. Darmenov¹, L. Dimitrov, V. Genchev¹, P. Iaydjiev,
S. Piperov, S. Stoykova, G. Sultanov, R. Trayanov, I. Vankov

University of Sofia, Sofia, Bulgaria

A. Dimitrov, M. Dyulendarova, V. Kozuharov, L. Litov, E. Marinova, M. Mateev, B. Pavlov,
P. Petkov, Z. Toteva¹

Institute of High Energy Physics, Beijing, China

G.M. Chen, H.S. Chen, W. Guan, C.H. Jiang, D. Liang, B. Liu, X. Meng, J. Tao, J. Wang, Z. Wang,
Z. Xue, Z. Zhang

State Key Lab. of Nucl. Phys. and Tech., Peking University, Beijing, China

Y. Ban, J. Cai, Y. Ge, S. Guo, Z. Hu, Y. Mao, S.J. Qian, H. Teng, B. Zhu

Universidad de Los Andes, Bogota, Colombia

C. Avila, M. Baquero Ruiz, C.A. Carrillo Montoya, A. Gomez, B. Gomez Moreno, A.A. Ocampo
Rios, A.F. Osorio Oliveros, D. Reyes Romero, J.C. Sanabria

Technical University of Split, Split, Croatia

N. Godinovic, K. Lelas, R. Plestina, D. Polic, I. Puljak

University of Split, Split, Croatia

Z. Antunovic, M. Dzelalija

Institute Rudjer Boskovic, Zagreb, Croatia

V. Brigljevic, S. Duric, K. Kadija, S. Morovic

University of Cyprus, Nicosia, Cyprus

R. Fereos, M. Galanti, J. Mousa, A. Papadakis, F. Ptochos, P.A. Razis, D. Tsiaakkouri, Z. Zinonos

National Institute of Chemical Physics and Biophysics, Tallinn, Estonia

A. Hektor, M. Kadastik, K. Kannike, M. Müntel, M. Raidal, L. Rebane

Helsinki Institute of Physics, Helsinki, Finland

E. Anttila, S. Czellar, J. Häkkinen, A. Heikkinen, V. Karimäki, R. Kinnunen, J. Klem,
M.J. Kortelainen, T. Lampén, K. Lassila-Perini, S. Lehti, T. Lindén, P. Luukka, T. Mäenpää,
J. Nysten, E. Tuominen, J. Tuominiemi, D. Ungaro, L. Wendland

Lappeenranta University of Technology, Lappeenranta, Finland

K. Banzuzi, A. Korpela, T. Tuuva

**Laboratoire d'Annecy-le-Vieux de Physique des Particules, IN2P3-CNRS, Annecy-le-Vieux,
France**

P. Nedelec, D. Sillou

DSM/IRFU, CEA/Saclay, Gif-sur-Yvette, France

M. Besancon, R. Chipaux, M. Dejardin, D. Denegri, J. Descamps, B. Fabbro, J.L. Faure, F. Ferri,
S. Ganjour, F.X. Gentit, A. Givernaud, P. Gras, G. Hamel de Monchenault, P. Jarry, M.C. Lemaire,
E. Locci, J. Malcles, M. Marionneau, L. Millischer, J. Rander, A. Rosowsky, D. Rousseau,
M. Titov, P. Verrecchia

Laboratoire Leprince-Ringuet, Ecole Polytechnique, IN2P3-CNRS, Palaiseau, France

S. Baffioni, L. Bianchini, M. Bluj³, P. Busson, C. Charlot, L. Dobrzynski, R. Granier de
Cassagnac, M. Haguenauer, P. Miné, P. Paganini, Y. Sirois, C. Thiebaux, A. Zabi

Institut Pluridisciplinaire Hubert Curien, Université de Strasbourg, Université de Haute Alsace Mulhouse, CNRS/IN2P3, Strasbourg, France

J.-L. Agram⁴, A. Besson, D. Bloch, D. Bodin, J.-M. Brom, E. Conte⁴, F. Drouhin⁴, J.-C. Fontaine⁴, D. Gelé, U. Goerlach, L. Gross, P. Juillot, A.-C. Le Bihan, Y. Patois, J. Speck, P. Van Hove

Université de Lyon, Université Claude Bernard Lyon 1, CNRS-IN2P3, Institut de Physique Nucléaire de Lyon, Villeurbanne, France

C. Baty, M. Bedjidian, J. Blaha, G. Boudoul, H. Brun, N. Chanon, R. Chierici, D. Contardo, P. Depasse, T. Dupasquier, H. El Mamouni, F. Fassi⁵, J. Fay, S. Gascon, B. Ille, T. Kurca, T. Le Grand, M. Lethuillier, N. Lumb, L. Mirabito, S. Perries, M. Vander Donckt, P. Verdier

E. Andronikashvili Institute of Physics, Academy of Science, Tbilisi, Georgia

N. Djaoshvili, N. Roinishvili, V. Roinishvili

Institute of High Energy Physics and Informatization, Tbilisi State University, Tbilisi, Georgia

N. Amaglobeli

RWTH Aachen University, I. Physikalisches Institut, Aachen, Germany

R. Adolphi, G. Anagnostou, R. Brauer, W. Braunschweig, M. Edelhoff, H. Esser, L. Feld, W. Karpinski, A. Khomich, K. Klein, N. Mohr, A. Ostaptchouk, D. Pandoulas, G. Pierschel, F. Raupach, S. Schael, A. Schultz von Dratzig, G. Schwering, D. Sprenger, M. Thomas, M. Weber, B. Wittmer, M. Wlochal

RWTH Aachen University, III. Physikalisches Institut A, Aachen, Germany

O. Actis, G. Altenhöfer, W. Bender, P. Biallass, M. Erdmann, G. Fetchenhauer¹, J. Frangenheim, T. Hebbeker, G. Hilgers, A. Hinzmann, K. Hoepfner, C. Hof, M. Kirsch, T. Klimkovich, P. Kreuzer¹, D. Lanske[†], M. Merschmeyer, A. Meyer, B. Philipps, H. Pieta, H. Reithler, S.A. Schmitz, L. Sonnenschein, M. Sowa, J. Steggemann, H. Szczesny, D. Teyssier, C. Zeidler

RWTH Aachen University, III. Physikalisches Institut B, Aachen, Germany

M. Bontenackels, M. Davids, M. Duda, G. Flügge, H. Geenen, M. Giffels, W. Haj Ahmad, T. Hermanns, D. Heydhausen, S. Kalinin, T. Kress, A. Linn, A. Nowack, L. Perchalla, M. Poettgens, O. Pooth, P. Sauerland, A. Stahl, D. Tornier, M.H. Zoeller

Deutsches Elektronen-Synchrotron, Hamburg, Germany

M. Aldaya Martin, U. Behrens, K. Borras, A. Campbell, E. Castro, D. Dammann, G. Eckerlin, A. Flossdorf, G. Flucke, A. Geiser, D. Hatton, J. Hauk, H. Jung, M. Kasemann, I. Katkov, C. Kleinwort, H. Kluge, A. Knutsson, E. Kuznetsova, W. Lange, W. Lohmann, R. Mankel¹, M. Marienfeld, A.B. Meyer, S. Miglioranzi, J. Mnich, M. Ohlerich, J. Olzem, A. Parenti, C. Rosemann, R. Schmidt, T. Schoerner-Sadenius, D. Volyansky, C. Wissing, W.D. Zeuner¹

University of Hamburg, Hamburg, Germany

C. Autermann, F. Bechtel, J. Draeger, D. Eckstein, U. Gebbert, K. Kaschube, G. Kaussen, R. Klanner, B. Mura, S. Naumann-Emme, F. Nowak, U. Pein, C. Sander, P. Schleper, T. Schum, H. Stadie, G. Steinbrück, J. Thomsen, R. Wolf

Institut für Experimentelle Kernphysik, Karlsruhe, Germany

J. Bauer, P. Blüm, V. Buege, A. Cakir, T. Chwalek, W. De Boer, A. Dierlamm, G. Dirkes, M. Feindt, U. Felzmann, M. Frey, A. Furgeri, J. Gruschke, C. Hackstein, F. Hartmann¹, S. Heier, M. Heinrich, H. Held, D. Hirschbuehl, K.H. Hoffmann, S. Honc, C. Jung, T. Kuhr, T. Liamsuwan, D. Martschei, S. Mueller, Th. Müller, M.B. Neuland, M. Niegel, O. Oberst, A. Oehler, J. Ott, T. Peiffer, D. Piparo, G. Quast, K. Rabbertz, F. Ratnikov, N. Ratnikova, M. Renz, C. Saout¹, G. Sartisohn, A. Scheurer, P. Schieferdecker, F.-P. Schilling, G. Schott, H.J. Simonis,

F.M. Stober, P. Sturm, D. Troendle, A. Trunov, W. Wagner, J. Wagner-Kuhr, M. Zeise, V. Zhukov⁶, E.B. Ziebarth

Institute of Nuclear Physics "Demokritos", Aghia Paraskevi, Greece

G. Daskalakis, T. Geralis, K. Karafasoulis, A. Kyriakis, D. Loukas, A. Markou, C. Markou, C. Mavrommatis, E. Petrakou, A. Zachariadou

University of Athens, Athens, Greece

L. Gouskos, P. Katsas, A. Panagiotou¹

University of Ioánnina, Ioánnina, Greece

I. Evangelou, P. Kokkas, N. Manthos, I. Papadopoulos, V. Patras, F.A. Triantis

KFKI Research Institute for Particle and Nuclear Physics, Budapest, Hungary

G. Bencze¹, L. Boldizsar, G. Debreczeni, C. Hajdu¹, S. Hernath, P. Hidas, D. Horvath⁷, K. Krajczar, A. Laszlo, G. Patay, F. Sikler, N. Toth, G. Vesztregombi

Institute of Nuclear Research ATOMKI, Debrecen, Hungary

N. Beni, G. Christian, J. Imrek, J. Molnar, D. Novak, J. Palinkas, G. Szekely, Z. Szillasi¹, K. Tokesi, V. Veszpremi

University of Debrecen, Debrecen, Hungary

A. Kapusi, G. Marian, P. Raics, Z. Szabo, Z.L. Trocsanyi, B. Ujvari, G. Zilizi

Panjab University, Chandigarh, India

S. Bansal, H.S. Bawa, S.B. Beri, V. Bhatnagar, M. Jindal, M. Kaur, R. Kaur, J.M. Kohli, M.Z. Mehta, N. Nishu, L.K. Saini, A. Sharma, A. Singh, J.B. Singh, S.P. Singh

University of Delhi, Delhi, India

S. Ahuja, S. Arora, S. Bhattacharya⁸, S. Chauhan, B.C. Choudhary, P. Gupta, S. Jain, S. Jain, M. Jha, A. Kumar, K. Ranjan, R.K. Shivpuri, A.K. Srivastava

Bhabha Atomic Research Centre, Mumbai, India

R.K. Choudhury, D. Dutta, S. Kailas, S.K. Kataria, A.K. Mohanty, L.M. Pant, P. Shukla, A. Topkar

Tata Institute of Fundamental Research - EHEP, Mumbai, India

T. Aziz, M. Guchait⁹, A. Gurtu, M. Maity¹⁰, D. Majumder, G. Majumder, K. Mazumdar, A. Nayak, A. Saha, K. Sudhakar

Tata Institute of Fundamental Research - HECR, Mumbai, India

S. Banerjee, S. Dugad, N.K. Mondal

Institute for Studies in Theoretical Physics & Mathematics (IPM), Tehran, Iran

H. Arfaei, H. Bakhshiansohi, A. Fahim, A. Jafari, M. Mohammadi Najafabadi, A. Moshaii, S. Pakhtinat Mehdiabadi, S. Rouhani, B. Safarzadeh, M. Zeinali

University College Dublin, Dublin, Ireland

M. Felcini

INFN Sezione di Bari ^a, Università di Bari ^b, Politecnico di Bari ^c, Bari, Italy

M. Abbrescia^{a,b}, L. Barbone^a, F. Chiumarulo^a, A. Clemente^a, A. Colaleo^a, D. Creanza^{a,c}, G. Cuscela^a, N. De Filippis^a, M. De Palma^{a,b}, G. De Robertis^a, G. Donvito^a, F. Fedele^a, L. Fiore^a, M. Franco^a, G. Iaselli^{a,c}, N. Lacalamita^a, F. Loddo^a, L. Lusito^{a,b}, G. Maggi^{a,c}, M. Maggi^a, N. Manna^{a,b}, B. Marangelli^{a,b}, S. My^{a,c}, S. Natali^{a,b}, S. Nuzzo^{a,b}, G. Papagni^a, S. Piccolomo^a, G.A. Pierro^a, C. Pinto^a, A. Pompili^{a,b}, G. Pugliese^{a,c}, R. Rajan^a, A. Ranieri^a, F. Romano^{a,c}

G. Roselli^{a,b}, G. Selvaggi^{a,b}, Y. Shinde^a, L. Silvestris^a, S. Tupputi^{a,b}, G. Zito^a

INFN Sezione di Bologna ^a, Universita di Bologna ^b, Bologna, Italy

G. Abbiendi^a, W. Bacchi^{a,b}, A.C. Benvenuti^a, M. Boldini^a, D. Bonacorsi^a, S. Braibant-Giacomelli^{a,b}, V.D. Cafaro^a, S.S. Caiazza^a, P. Capiluppi^{a,b}, A. Castro^{a,b}, F.R. Cavallo^a, G. Codispoti^{a,b}, M. Cuffiani^{a,b}, I. D'Antone^a, G.M. Dallavalle^{a,1}, F. Fabbri^a, A. Fanfani^{a,b}, D. Fasanella^a, P. Giacomelli^a, V. Giordano^a, M. Giunta^{a,1}, C. Grandi^a, M. Guerzoni^a, S. Marcellini^a, G. Masetti^{a,b}, A. Montanari^a, F.L. Navarria^{a,b}, F. Odorici^a, G. Pellegrini^a, A. Perrotta^a, A.M. Rossi^{a,b}, T. Rovelli^{a,b}, G. Siroli^{a,b}, G. Torromeo^a, R. Travaglini^{a,b}

INFN Sezione di Catania ^a, Universita di Catania ^b, Catania, Italy

S. Albergo^{a,b}, S. Costa^{a,b}, R. Potenza^{a,b}, A. Tricomi^{a,b}, C. Tuve^a

INFN Sezione di Firenze ^a, Universita di Firenze ^b, Firenze, Italy

G. Barbagli^a, G. Broccolo^{a,b}, V. Ciulli^{a,b}, C. Civinini^a, R. D'Alessandro^{a,b}, E. Focardi^{a,b}, S. Frosali^{a,b}, E. Gallo^a, C. Genta^{a,b}, G. Landi^{a,b}, P. Lenzi^{a,b,1}, M. Meschini^a, S. Paoletti^a, G. Sguazzoni^a, A. Tropiano^a

INFN Laboratori Nazionali di Frascati, Frascati, Italy

L. Benussi, M. Bertani, S. Bianco, S. Colafranceschi¹¹, D. Colonna¹¹, F. Fabbri, M. Giardoni, L. Passamonti, D. Piccolo, D. Pierluigi, B. Ponzio, A. Russo

INFN Sezione di Genova, Genova, Italy

P. Fabbricatore, R. Musenich

INFN Sezione di Milano-Biccoca ^a, Universita di Milano-Bicocca ^b, Milano, Italy

A. Benaglia^a, M. Calloni^a, G.B. Cerati^{a,b,1}, P. D'Angelo^a, F. De Guio^a, F.M. Farina^a, A. Ghezzi^a, P. Govoni^{a,b}, M. Malberti^{a,b,1}, S. Malvezzi^a, A. Martelli^a, D. Menasce^a, V. Miccio^{a,b}, L. Moroni^a, P. Negri^{a,b}, M. Paganoni^{a,b}, D. Pedrini^a, A. Pullia^{a,b}, S. Ragazzi^{a,b}, N. Redaelli^a, S. Sala^a, R. Salerno^{a,b}, T. Tabarelli de Fatis^{a,b}, V. Tancini^{a,b}, S. Taroni^{a,b}

INFN Sezione di Napoli ^a, Universita di Napoli "Federico II" ^b, Napoli, Italy

S. Buontempo^a, N. Cavallo^a, A. Cimmino^{a,b,1}, M. De Gruttola^{a,b,1}, F. Fabozzi^{a,12}, A.O.M. Iorio^a, L. Lista^a, D. Lomidze^a, P. Noli^{a,b}, P. Paolucci^a, C. Sciacca^{a,b}

INFN Sezione di Padova ^a, Università di Padova ^b, Padova, Italy

P. Azzi^{a,1}, N. Bacchetta^a, L. Barcellan^a, P. Bellan^{a,b,1}, M. Bellato^a, M. Benettoni^a, M. Biasotto^{a,13}, D. Bisello^{a,b}, E. Borsato^{a,b}, A. Branca^a, R. Carlin^{a,b}, L. Castellani^a, P. Checchia^a, E. Conti^a, F. Dal Corso^a, M. De Mattia^{a,b}, T. Dorigo^a, U. Dosselli^a, F. Fanzago^a, F. Gasparini^{a,b}, U. Gasparini^{a,b}, P. Giubilato^{a,b}, F. Gonella^a, A. Gresele^{a,14}, M. Gulmini^{a,13}, A. Kaminsky^{a,b}, S. Lacaprara^{a,13}, I. Lazzizzera^{a,14}, M. Margoni^{a,b}, G. Maron^{a,13}, S. Mattiazzo^{a,b}, M. Mazzucato^a, M. Meneghelli^a, A.T. Meneguzzo^{a,b}, M. Michelotto^a, F. Montecassiano^a, M. Nespolo^a, M. Passaseo^a, M. Pegoraro^a, L. Perrozzi^a, N. Pozzobon^{a,b}, P. Ronchese^{a,b}, F. Simonetto^{a,b}, N. Toniolo^a, E. Torassa^a, M. Tosi^{a,b}, A. Triassi^a, S. Vanini^{a,b}, S. Ventura^a, P. Zotto^{a,b}, G. Zumerle^{a,b}

INFN Sezione di Pavia ^a, Universita di Pavia ^b, Pavia, Italy

P. Baesso^{a,b}, U. Berzano^a, S. Bricola^a, M.M. Necchi^{a,b}, D. Pagano^{a,b}, S.P. Ratti^{a,b}, C. Riccardi^{a,b}, P. Torre^{a,b}, A. Vicini^a, P. Vitulo^{a,b}, C. Viviani^{a,b}

INFN Sezione di Perugia ^a, Universita di Perugia ^b, Perugia, Italy

D. Aisa^a, S. Aisa^a, E. Babucci^a, M. Biasini^{a,b}, G.M. Bilei^a, B. Caponeri^{a,b}, B. Checcucci^a, N. Dinu^a, L. Fanò^a, L. Farnesini^a, P. Lariccia^{a,b}, A. Lucaroni^{a,b}, G. Mantovani^{a,b}, A. Nappi^{a,b}, A. Piluso^a, V. Postolache^a, A. Santocchia^{a,b}, L. Servoli^a, D. Tonello^a, A. Vedaee^a, R. Volpe^{a,b}

INFN Sezione di Pisa ^a, Universita di Pisa ^b, Scuola Normale Superiore di Pisa ^c, Pisa, Italy
 P. Azzurri^{a,c}, G. Bagliesi^a, J. Bernardini^{a,b}, L. Berretta^a, T. Boccali^a, A. Bocci^{a,c}, L. Borrello^{a,c}, F. Bosi^a, F. Calzolari^a, R. Castaldi^a, R. Dell'Orso^a, F. Fiori^{a,b}, L. Foà^{a,c}, S. Gennai^{a,c}, A. Giassi^a, A. Kraan^a, F. Ligabue^{a,c}, T. Lomtadze^a, F. Mariani^a, L. Martini^a, M. Massa^a, A. Messineo^{a,b}, A. Moggi^a, F. Palla^a, F. Palmonari^a, G. Petragnani^a, G. Petrisciani^{a,c}, F. Raffaelli^a, S. Sarkar^a, G. Segneri^a, A.T. Serban^a, P. Spagnolo^{a,1}, R. Tenchini^{a,1}, S. Tolaini^a, G. Tonelli^{a,b,1}, A. Venturi^a, P.G. Verdini^a

INFN Sezione di Roma ^a, Universita di Roma "La Sapienza" ^b, Roma, Italy

S. Baccaro^{a,15}, L. Barone^{a,b}, A. Bartoloni^a, F. Cavallari^{a,1}, I. Dafinei^a, D. Del Re^{a,b}, E. Di Marco^{a,b}, M. Diemoz^a, D. Franci^{a,b}, E. Longo^{a,b}, G. Organtini^{a,b}, A. Palma^{a,b}, F. Pandolfi^{a,b}, R. Paramatti^{a,1}, F. Pellegrino^a, S. Rahatlou^{a,b}, C. Rovelli^a

INFN Sezione di Torino ^a, Università di Torino ^b, Università del Piemonte Orientale (Novara) ^c, Torino, Italy

G. Alampi^a, N. Amapane^{a,b}, R. Arcidiacono^{a,b}, S. Argiro^{a,b}, M. Arneodo^{a,c}, C. Biino^a, M.A. Borgia^{a,b}, C. Botta^{a,b}, N. Cartiglia^a, R. Castello^{a,b}, G. Cerminara^{a,b}, M. Costa^{a,b}, D. Dattola^a, G. Dellacasa^a, N. Demaria^a, G. Dughera^a, F. Dumitrache^a, A. Graziano^{a,b}, C. Mariotti^a, M. Marone^{a,b}, S. Maselli^a, E. Migliore^{a,b}, G. Mila^{a,b}, V. Monaco^{a,b}, M. Musich^{a,b}, M. Nervo^{a,b}, M.M. Obertino^{a,c}, S. Oggero^{a,b}, R. Panero^a, N. Pastrone^a, M. Pelliccioni^{a,b}, A. Romero^{a,b}, M. Ruspa^{a,c}, R. Sacchi^{a,b}, A. Solano^{a,b}, A. Staiano^a, P.P. Trapani^{a,b,1}, D. Trocino^{a,b}, A. Vilela Pereira^{a,b}, L. Visca^{a,b}, A. Zampieri^a

INFN Sezione di Trieste ^a, Universita di Trieste ^b, Trieste, Italy

F. Ambroglini^{a,b}, S. Belforte^a, F. Cossutti^a, G. Della Ricca^{a,b}, B. Gobbo^a, A. Penzo^a

Kyungpook National University, Daegu, Korea

S. Chang, J. Chung, D.H. Kim, G.N. Kim, D.J. Kong, H. Park, D.C. Son

Wonkwang University, Iksan, Korea

S.Y. Bahk

Chonnam National University, Kwangju, Korea

S. Song

Konkuk University, Seoul, Korea

S.Y. Jung

Korea University, Seoul, Korea

B. Hong, H. Kim, J.H. Kim, K.S. Lee, D.H. Moon, S.K. Park, H.B. Rhee, K.S. Sim

Seoul National University, Seoul, Korea

J. Kim

University of Seoul, Seoul, Korea

M. Choi, G. Hahn, I.C. Park

Sungkyunkwan University, Suwon, Korea

S. Choi, Y. Choi, J. Goh, H. Jeong, T.J. Kim, J. Lee, S. Lee

Vilnius University, Vilnius, Lithuania

M. Janulis, D. Martisiute, P. Petrov, T. Sabonis

Centro de Investigacion y de Estudios Avanzados del IPN, Mexico City, Mexico

H. Castilla Valdez¹, A. Sánchez Hernández

Universidad Iberoamericana, Mexico City, Mexico

S. Carrillo Moreno

Universidad Autónoma de San Luis Potosí, San Luis Potosí, Mexico

A. Morelos Pineda

University of Auckland, Auckland, New Zealand

P. Allfrey, R.N.C. Gray, D. Kroccheck

University of Canterbury, Christchurch, New Zealand

N. Bernardino Rodrigues, P.H. Butler, T. Signal, J.C. Williams

National Centre for Physics, Quaid-I-Azam University, Islamabad, Pakistan

M. Ahmad, I. Ahmed, W. Ahmed, M.I. Asghar, M.I.M. Awan, H.R. Hoorani, I. Hussain, W.A. Khan, T. Khurshid, S. Muhammad, S. Qazi, H. Shahzad

Institute of Experimental Physics, Warsaw, PolandM. Cwiok, R. Dabrowski, W. Dominik, K. Doroba, M. Konecki, J. Krolikowski, K. Pozniak¹⁶, R. Romaniuk, W. Zabolotny¹⁶, P. Zych**Soltan Institute for Nuclear Studies, Warsaw, Poland**

T. Frueboes, R. Gokieli, L. Goscilo, M. Górski, M. Kazana, K. Nawrocki, M. Szleper, G. Wrochna, P. Zalewski

Laboratório de Instrumentação e Física Experimental de Partículas, Lisboa, Portugal

N. Almeida, L. Antunes Pedro, P. Bargassa, A. David, P. Faccioli, P.G. Ferreira Parracho, M. Freitas Ferreira, M. Gallinaro, M. Guerra Jordao, P. Martins, G. Mini, P. Musella, J. Pela, L. Raposo, P.Q. Ribeiro, S. Sampaio, J. Seixas, J. Silva, P. Silva, D. Soares, M. Sousa, J. Varela, H.K. Wöhri

Joint Institute for Nuclear Research, Dubna, Russia

I. Altsybeev, I. Belotelov, P. Bunin, Y. Ershov, I. Filozova, M. Finger, M. Finger Jr., A. Golunov, I. Golutvin, N. Gorbounov, V. Kalagin, A. Kamenev, V. Karjavin, V. Konoplyanikov, V. Korenkov, G. Kozlov, A. Kurenkov, A. Lanev, A. Makankin, V.V. Mitsyn, P. Moisenz, E. Nikonov, D. Oleynik, V. Palichik, V. Perelygin, A. Petrosyan, R. Semenov, S. Shmatov, V. Smirnov, D. Smolin, E. Tikhonenko, S. Vasil'ev, A. Vishnevskiy, A. Volodko, A. Zarubin, V. Zhiltsov

Petersburg Nuclear Physics Institute, Gatchina (St Petersburg), Russia

N. Bondar, L. Chtchipounov, A. Denisov, Y. Gavrikov, G. Gavrilov, V. Golovtsov, Y. Ivanov, V. Kim, V. Kozlov, P. Levchenko, G. Obrant, E. Orishchin, A. Petrunin, Y. Shcheglov, A. Shchetkovskiy, V. Sknar, I. Smirnov, V. Sulimov, V. Tarakanov, L. Uvarov, S. Vavilov, G. Velichko, S. Volkov, A. Vorobyev

Institute for Nuclear Research, Moscow, Russia

Yu. Andreev, A. Anisimov, P. Antipov, A. Dermenev, S. Gninenko, N. Golubev, M. Kirsanov, N. Krasnikov, V. Matveev, A. Pashenkov, V.E. Postoev, A. Solovey, A. Solovey, A. Toropin, S. Troitsky

Institute for Theoretical and Experimental Physics, Moscow, RussiaA. Baud, V. Epshteyn, V. Gavrilov, N. Ilina, V. Kaftanov[†], V. Kolosov, M. Kossov¹, A. Krokhitin, S. Kuleshov, A. Oulianov, G. Safronov, S. Semenov, I. Shreyber, V. Stolin, E. Vlasov, A. Zhokin**Moscow State University, Moscow, Russia**E. Boos, M. Dubinin¹⁷, L. Dudko, A. Ershov, A. Gribushin, V. Klyukhin, O. Kodolova, I. Loktin,

S. Petrushanko, L. Sarycheva, V. Savrin, A. Snigirev, I. Vardanyan

P.N. Lebedev Physical Institute, Moscow, Russia

I. Dremin, M. Kirakosyan, N. Konovalova, S.V. Rusakov, A. Vinogradov

State Research Center of Russian Federation, Institute for High Energy Physics, Protvino, Russia

S. Akimenko, A. Artamonov, I. Azhgirey, S. Bitioukov, V. Burtovoy, V. Grishin¹, V. Kachanov, D. Konstantinov, V. Krychkine, A. Levine, I. Lobov, V. Lukin, Y. Mel'nik, V. Petrov, R. Ryutin, S. Slabospitsky, A. Sobol, A. Sytine, L. Tourtchanovitch, S. Troshin, N. Tyurin, A. Uzunian, A. Volkov

Vinca Institute of Nuclear Sciences, Belgrade, Serbia

P. Adzic, M. Djordjevic, D. Jovanovic¹⁸, D. Krpic¹⁸, D. Maletic, J. Puzovic¹⁸, N. Smiljkovic

Centro de Investigaciones Energéticas Medioambientales y Tecnológicas (CIEMAT), Madrid, Spain

M. Aguilar-Benitez, J. Alberdi, J. Alcaraz Maestre, P. Arce, J.M. Barcala, C. Battilana, C. Burgos Lazaro, J. Caballero Bejar, E. Calvo, M. Cardenas Montes, M. Cepeda, M. Cerrada, M. Chamizo Llatas, F. Clemente, N. Colino, M. Daniel, B. De La Cruz, A. Delgado Peris, C. Diez Pardos, C. Fernandez Bedoya, J.P. Fernández Ramos, A. Ferrando, J. Flix, M.C. Fouz, P. Garcia-Abia, A.C. Garcia-Bonilla, O. Gonzalez Lopez, S. Goy Lopez, J.M. Hernandez, M.I. Josa, J. Marin, G. Merino, J. Molina, A. Molinero, J.J. Navarrete, J.C. Oller, J. Puerta Pelayo, L. Romero, J. Santaolalla, C. Villanueva Munoz, C. Willmott, C. Yuste

Universidad Autónoma de Madrid, Madrid, Spain

C. Albajar, M. Blanco Otano, J.F. de Trocóniz, A. Garcia Raboso, J.O. Lopez Berengueres

Universidad de Oviedo, Oviedo, Spain

J. Cuevas, J. Fernandez Menendez, I. Gonzalez Caballero, L. Lloret Iglesias, H. Naves Sordo, J.M. Vizan Garcia

Instituto de Física de Cantabria (IFCA), CSIC-Universidad de Cantabria, Santander, Spain

I.J. Cabrillo, A. Calderon, S.H. Chuang, I. Diaz Merino, C. Diez Gonzalez, J. Duarte Campderros, M. Fernandez, G. Gomez, J. Gonzalez Sanchez, R. Gonzalez Suarez, C. Jorda, P. Lobelle Pardo, A. Lopez Virto, J. Marco, R. Marco, C. Martinez Rivero, P. Martinez Ruiz del Arbol, F. Matorras, T. Rodrigo, A. Ruiz Jimeno, L. Scodellaro, M. Sobron Sanudo, I. Vila, R. Vilar Cortabitarte

CERN, European Organization for Nuclear Research, Geneva, Switzerland

D. Abbaneo, E. Albert, M. Alidra, S. Ashby, E. Auffray, J. Baechler, P. Baillon, A.H. Ball, S.L. Bally, D. Barney, F. Beaudette¹⁹, R. Bellan, D. Benedetti, G. Benelli, C. Bernet, P. Bloch, S. Bolognesi, M. Bona, J. Bos, N. Bourgeois, T. Bourrel, H. Breuker, K. Bunkowski, D. Campi, T. Camporesi, E. Cano, A. Cattai, J.P. Chatelain, M. Chauvey, T. Christiansen, J.A. Coarasa Perez, A. Conde Garcia, R. Covarelli, B. Curé, A. De Roeck, V. Delachenal, D. Deyrail, S. Di Vincenzo²⁰, S. Dos Santos, T. Dupont, L.M. Edera, A. Elliott-Peisert, M. Eppard, M. Favre, N. Frank, W. Funk, A. Gaddi, M. Gastal, M. Gateau, H. Gerwig, D. Gigi, K. Gill, D. Giordano, J.P. Girod, F. Glege, R. Gomez-Reino Garrido, R. Goudard, S. Gowdy, R. Guida, L. Guiducci, J. Gutleber, M. Hansen, C. Hartl, J. Harvey, B. Hegner, H.F. Hoffmann, A. Holzner, A. Honma, M. Huhtinen, V. Innocente, P. Janot, G. Le Godec, P. Lecoq, C. Leonidopoulos, R. Loos, C. Lourenço, A. Lyonnet, A. Macpherson, N. Magini, J.D. Maillefaud, G. Maire, T. Mäki, L. Malgeri, M. Mannelli, L. Masetti, F. Meijers, P. Meridiani, S. Mersi, E. Meschi, A. Meynet Cordonnier, R. Moser, M. Mulders, J. Mulon, M. Noy, A. Oh, G. Olesen, A. Onnela, T. Orimoto,

L. Orsini, E. Perez, G. Perinic, J.F. Pernot, P. Petagna, P. Petiot, A. Petrilli, A. Pfeiffer, M. Pierini, M. Pimiä, R. Pintus, B. Pirollet, H. Postema, A. Racz, S. Ravat, S.B. Rew, J. Rodrigues Antunes, G. Rolandi²¹, M. Rovere, V. Ryjov, H. Sakulin, D. Samyn, H. Sauce, C. Schäfer, W.D. Schlatter, M. Schröder, C. Schwick, A. Sciaba, I. Segoni, A. Sharma, N. Siegrist, P. Siegrist, N. Sinanis, T. Sobrier, P. Sphicas²², D. Spiga, M. Spiropulu¹⁷, F. Stöckli, P. Traczyk, P. Tropea, J. Troska, A. Tsirou, L. Veillet, G.I. Veres, M. Voutilainen, P. Wertelaers, M. Zanetti

Paul Scherrer Institut, Villigen, Switzerland

W. Bertl, K. Deiters, W. Erdmann, K. Gabathuler, R. Horisberger, Q. Ingram, H.C. Kaestli, S. König, D. Kotlinski, U. Langenegger, F. Meier, D. Renker, T. Rohe, J. Sibille²³, A. Starodumov²⁴

Institute for Particle Physics, ETH Zurich, Zurich, Switzerland

B. Betev, L. Caminada²⁵, Z. Chen, S. Cittolin, D.R. Da Silva Di Calafiori, S. Dambach²⁵, G. Dissertori, M. Dittmar, C. Eggel²⁵, J. Eugster, G. Faber, K. Freudenreich, C. Grab, A. Hervé, W. Hintz, P. Lecomte, P.D. Luckey, W. Lustermann, C. Marchica²⁵, P. Milenovic²⁶, F. Moortgat, A. Nardulli, F. Nessi-Tedaldi, L. Pape, F. Pauss, T. Punz, A. Rizzi, F.J. Ronga, L. Sala, A.K. Sanchez, M.-C. Sawley, V. Sordini, B. Stieger, L. Tauscher[†], A. Thea, K. Theofilatos, D. Treille, P. Trüb²⁵, M. Weber, L. Wehrli, J. Weng, S. Zelepoukine²⁷

Universität Zürich, Zurich, Switzerland

C. Amsler, V. Chiochia, S. De Visscher, C. Regenfus, P. Robmann, T. Rommerskirchen, A. Schmidt, D. Tsirikas, L. Wilke

National Central University, Chung-Li, Taiwan

Y.H. Chang, E.A. Chen, W.T. Chen, A. Go, C.M. Kuo, S.W. Li, W. Lin

National Taiwan University (NTU), Taipei, Taiwan

P. Bartalini, P. Chang, Y. Chao, K.F. Chen, W.-S. Hou, Y. Hsiung, Y.J. Lei, S.W. Lin, R.-S. Lu, J. Schümann, J.G. Shiu, Y.M. Tzeng, K. Ueno, Y. Velikzhanin, C.C. Wang, M. Wang

Cukurova University, Adana, Turkey

A. Adiguzel, A. Ayhan, A. Azman Gokce, M.N. Bakirci, S. Cerci, I. Dumanoglu, E. Eskut, S. Girgis, E. Gurpinar, I. Hos, T. Karaman, T. Karaman, A. Kayis Topaksu, P. Kurt, G. Önengüt, G. Önengüt Gökbüllüt, K. Ozdemir, S. Ozturk, A. Polatöz, K. Sogut²⁸, B. Tali, H. Topakli, D. Uzun, L.N. Vergili, M. Vergili

Middle East Technical University, Physics Department, Ankara, Turkey

I.V. Akin, T. Aliev, S. Bilmis, M. Deniz, H. Gamsizkan, A.M. Guler, K. Öcalan, M. Serin, R. Sever, U.E. Surat, M. Zeyrek

Bogaziçi University, Department of Physics, Istanbul, Turkey

M. Deliomeroglu, D. Demir²⁹, E. Gülmез, A. Halu, B. Isildak, M. Kaya³⁰, O. Kaya³⁰, S. Ozkorucuklu³¹, N. Sonmez³²

National Scientific Center, Kharkov Institute of Physics and Technology, Kharkov, Ukraine

L. Levchuk, S. Lukyanenko, D. Soroka, S. Zub

University of Bristol, Bristol, United Kingdom

F. Bostock, J.J. Brooke, T.L. Cheng, D. Cussans, R. Frazier, J. Goldstein, N. Grant, M. Hansen, G.P. Heath, H.F. Heath, C. Hill, B. Huckvale, J. Jackson, C.K. Mackay, S. Metson, D.M. Newbold³³, K. Nirunpong, V.J. Smith, J. Velthuis, R. Walton

Rutherford Appleton Laboratory, Didcot, United Kingdom

K.W. Bell, C. Brew, R.M. Brown, B. Camanzi, D.J.A. Cockerill, J.A. Coughlan, N.I. Geddes,

K. Harder, S. Harper, B.W. Kennedy, P. Murray, C.H. Shepherd-Themistocleous, I.R. Tomalin, J.H. Williams[†], W.J. Womersley, S.D. Worm

Imperial College, University of London, London, United Kingdom

R. Bainbridge, G. Ball, J. Ballin, R. Beuselinck, O. Buchmuller, D. Colling, N. Cripps, G. Davies, M. Della Negra, C. Foudas, J. Fulcher, D. Futyan, G. Hall, J. Hays, G. Iles, G. Karapostoli, B.C. MacEvoy, A.-M. Magnan, J. Marrouche, J. Nash, A. Nikitenko²⁴, A. Papageorgiou, M. Pesaresi, K. Petridis, M. Pioppi³⁴, D.M. Raymond, N. Rompotis, A. Rose, M.J. Ryan, C. Seez, P. Sharp, G. Sidiropoulos¹, M. Stettler, M. Stoye, M. Takahashi, A. Tapper, C. Timlin, S. Tourneur, M. Vazquez Acosta, T. Virdee¹, S. Wakefield, D. Wardrope, T. Whyntie, M. Wingham

Brunel University, Uxbridge, United Kingdom

J.E. Cole, I. Goitom, P.R. Hobson, A. Khan, P. Kyberd, D. Leslie, C. Munro, I.D. Reid, C. Siamitros, R. Taylor, L. Teodorescu, I. Yaselli

Boston University, Boston, USA

T. Bose, M. Carleton, E. Hazen, A.H. Heering, A. Heister, J. St. John, P. Lawson, D. Lazic, D. Osborne, J. Rohlf, L. Sulak, S. Wu

Brown University, Providence, USA

J. Andrea, A. Avetisyan, S. Bhattacharya, J.P. Chou, D. Cutts, S. Esen, G. Kukartsev, G. Landsberg, M. Narain, D. Nguyen, T. Speer, K.V. Tsang

University of California, Davis, Davis, USA

R. Breedon, M. Calderon De La Barca Sanchez, M. Case, D. Cebra, M. Chertok, J. Conway, P.T. Cox, J. Dolen, R. Erbacher, E. Friis, W. Ko, A. Kopecky, R. Lander, A. Lister, H. Liu, S. Maruyama, T. Miceli, M. Nikolic, D. Pellett, J. Robles, M. Searle, J. Smith, M. Squires, J. Stilley, M. Tripathi, R. Vasquez Sierra, C. Veelken

University of California, Los Angeles, Los Angeles, USA

V. Andreev, K. Arisaka, D. Cline, R. Cousins, S. Erhan¹, J. Hauser, M. Ignatenko, C. Jarvis, J. Mumford, C. Plager, G. Rakness, P. Schlein[†], J. Tucker, V. Valuev, R. Wallny, X. Yang

University of California, Riverside, Riverside, USA

J. Babb, M. Bose, A. Chandra, R. Clare, J.A. Ellison, J.W. Gary, G. Hanson, G.Y. Jeng, S.C. Kao, F. Liu, H. Liu, A. Luthra, H. Nguyen, G. Pasztor³⁵, A. Satpathy, B.C. Shen[†], R. Stringer, J. Sturdy, V. Sytnik, R. Wilken, S. Wimpenny

University of California, San Diego, La Jolla, USA

J.G. Branson, E. Dusinberre, D. Evans, F. Golf, R. Kelley, M. Lebourgeois, J. Letts, E. Lipeles, B. Mangano, J. Muelmenstaedt, M. Norman, S. Padhi, A. Petrucci, H. Pi, M. Pieri, R. Ranieri, M. Sani, V. Sharma, S. Simon, F. Würthwein, A. Yagil

University of California, Santa Barbara, Santa Barbara, USA

C. Campagnari, M. D'Alfonso, T. Danielson, J. Garberson, J. Incandela, C. Justus, P. Kalavase, S.A. Koay, D. Kovalevskyi, V. Krutelyov, J. Lamb, S. Lowette, V. Pavlunin, F. Rebassoo, J. Ribnik, J. Richman, R. Rossin, D. Stuart, W. To, J.R. Vlimant, M. Witherell

California Institute of Technology, Pasadena, USA

A. Apresyan, A. Bornheim, J. Bunn, M. Chiorboli, M. Gataullin, D. Kcira, V. Litvine, Y. Ma, H.B. Newman, C. Rogan, V. Timciuc, J. Veverka, R. Wilkinson, Y. Yang, L. Zhang, K. Zhu, R.Y. Zhu

Carnegie Mellon University, Pittsburgh, USA

B. Akgun, R. Carroll, T. Ferguson, D.W. Jang, S.Y. Jun, M. Paulini, J. Russ, N. Terentyev, H. Vogel, I. Vorobiev

University of Colorado at Boulder, Boulder, USA

J.P. Cumalat, M.E. Dinardo, B.R. Drell, W.T. Ford, B. Heyburn, E. Luiggi Lopez, U. Nauenberg, K. Stenson, K. Ulmer, S.R. Wagner, S.L. Zang

Cornell University, Ithaca, USA

L. Agostino, J. Alexander, F. Blekman, D. Cassel, A. Chatterjee, S. Das, L.K. Gibbons, B. Heltsley, W. Hopkins, A. Khukhunaishvili, B. Kreis, V. Kuznetsov, J.R. Patterson, D. Puigh, A. Ryd, X. Shi, S. Stroiney, W. Sun, W.D. Teo, J. Thom, J. Vaughan, Y. Weng, P. Wittich

Fairfield University, Fairfield, USA

C.P. Beetz, G. Cirino, C. Sanzeni, D. Winn

Fermi National Accelerator Laboratory, Batavia, USA

S. Abdullin, M.A. Afaq¹, M. Albrow, B. Ananthan, G. Apollinari, M. Atac, W. Badgett, L. Bagby, J.A. Bakken, B. Baldin, S. Banerjee, K. Banicz, L.A.T. Bauerdick, A. Beretvas, J. Berryhill, P.C. Bhat, K. Biery, M. Binkley, I. Bloch, F. Borcherding, A.M. Brett, K. Burkett, J.N. Butler, V. Chetluru, H.W.K. Cheung, F. Chlebana, I. Churin, S. Cihangir, M. Crawford, W. Dagenhart, M. Demarteau, G. Derylo, D. Dykstra, D.P. Eartly, J.E. Elias, V.D. Elvira, D. Evans, L. Feng, M. Fischler, I. Fisk, S. Foulkes, J. Freeman, P. Gartung, E. Gottschalk, T. Grassi, D. Green, Y. Guo, O. Gutsche, A. Hahn, J. Hanlon, R.M. Harris, B. Holzman, J. Howell, D. Hufnagel, E. James, H. Jensen, M. Johnson, C.D. Jones, U. Joshi, E. Juska, J. Kaiser, B. Klima, S. Kossiakov, K. Kousouris, S. Kwan, C.M. Lei, P. Limon, J.A. Lopez Perez, S. Los, L. Lueking, G. Lukhanin, S. Lusin¹, J. Lykken, K. Maeshima, J.M. Marraffino, D. Mason, P. McBride, T. Miao, K. Mishra, S. Moccia, R. Mommsen, S. Mrenna, A.S. Muhammad, C. Newman-Holmes, C. Noeding, V. O'Dell, O. Prokofyev, R. Rivera, C.H. Rivetta, A. Ronzhin, P. Rossman, S. Ryu, V. Sekhri, E. Sexton-Kennedy, I. Sfiligoi, S. Sharma, T.M. Shaw, D. Shpakov, E. Skup, R.P. Smith[†], A. Soha, W.J. Spalding, L. Spiegel, I. Suzuki, P. Tan, W. Tanenbaum, S. Tkaczyk¹, R. Trentadue¹, L. Uplegger, E.W. Vaandering, R. Vidal, J. Whitmore, E. Wicklund, W. Wu, J. Yarba, F. Yumiceva, J.C. Yun

University of Florida, Gainesville, USA

D. Acosta, P. Avery, V. Barashko, D. Bourilkov, M. Chen, G.P. Di Giovanni, D. Dobur, A. Drozdetskiy, R.D. Field, Y. Fu, I.K. Furic, J. Gartner, D. Holmes, B. Kim, S. Klimenko, J. Konigsberg, A. Korytov, K. Kotov, A. Kropivnitskaya, T. Kypreos, A. Madorsky, K. Matchev, G. Mitselmakher, Y. Pakhotin, J. Piedra Gomez, C. Prescott, V. Rapsevicius, R. Remington, M. Schmitt, B. Scurlock, D. Wang, J. Yelton

Florida International University, Miami, USA

C. Ceron, V. Gaultney, L. Kramer, L.M. Lebolo, S. Linn, P. Markowitz, G. Martinez, J.L. Rodriguez

Florida State University, Tallahassee, USA

T. Adams, A. Askew, H. Baer, M. Bertoldi, J. Chen, W.G.D. Dharmaratna, S.V. Gleyzer, J. Haas, S. Hagopian, V. Hagopian, M. Jenkins, K.F. Johnson, E. Prettner, H. Prosper, S. Sekmen

Florida Institute of Technology, Melbourne, USA

M.M. Baarmann, S. Guragain, M. Hohlmann, H. Kalakhety, H. Mermerkaya, R. Ralich, I. Vodopiyanova

University of Illinois at Chicago (UIC), Chicago, USA

B. Abelev, M.R. Adams, I.M. Anghel, L. Apanasevich, V.E. Bazterra, R.R. Betts, J. Callner,

M.A. Castro, R. Cavanaugh, C. Dragoiu, E.J. Garcia-Solis, C.E. Gerber, D.J. Hofman, S. Khalatian, C. Mironov, E. Shabalina, A. Smoron, N. Varelas

The University of Iowa, Iowa City, USA

U. Akgun, E.A. Albayrak, A.S. Ayan, B. Bilki, R. Briggs, K. Cankocak³⁶, K. Chung, W. Clarida, P. Debbins, F. Duru, F.D. Ingram, C.K. Lae, E. McCliment, J.-P. Merlo, A. Mestvirishvili, M.J. Miller, A. Moeller, J. Nachtman, C.R. Newsom, E. Norbeck, J. Olson, Y. Onel, F. Ozok, J. Parsons, I. Schmidt, S. Sen, J. Wetzel, T. Yetkin, K. Yi

Johns Hopkins University, Baltimore, USA

B.A. Barnett, B. Blumenfeld, A. Bonato, C.Y. Chien, D. Fehling, G. Giurgiu, A.V. Gritsan, Z.J. Guo, P. Maksimovic, S. Rappoccio, M. Swartz, N.V. Tran, Y. Zhang

The University of Kansas, Lawrence, USA

P. Baringer, A. Bean, O. Grachov, M. Murray, V. Radicci, S. Sanders, J.S. Wood, V. Zhukova

Kansas State University, Manhattan, USA

D. Bandurin, T. Bolton, K. Kaadze, A. Liu, Y. Maravin, D. Onoprienko, I. Svintradze, Z. Wan

Lawrence Livermore National Laboratory, Livermore, USA

J. Gronberg, J. Hollar, D. Lange, D. Wright

University of Maryland, College Park, USA

D. Baden, R. Bard, M. Boutemeur, S.C. Eno, D. Ferencek, N.J. Hadley, R.G. Kellogg, M. Kirn, S. Kunori, K. Rossato, P. Rumerio, F. Santanastasio, A. Skuja, J. Temple, M.B. Tonjes, S.C. Tonwar, T. Toole, E. Twedt

Massachusetts Institute of Technology, Cambridge, USA

B. Alver, G. Bauer, J. Bendavid, W. Busza, E. Butz, I.A. Cali, M. Chan, D. D'Enterria, P. Everaerts, G. Gomez Ceballos, K.A. Hahn, P. Harris, S. Jaditz, Y. Kim, M. Klute, Y.-J. Lee, W. Li, C. Loizides, T. Ma, M. Miller, S. Nahn, C. Paus, C. Roland, G. Roland, M. Rudolph, G. Stephans, K. Sumorok, K. Sung, S. Vaurynovich, E.A. Wenger, B. Wyslouch, S. Xie, Y. Yilmaz, A.S. Yoon

University of Minnesota, Minneapolis, USA

D. Bailleux, S.I. Cooper, P. Cushman, B. Dahmes, A. De Benedetti, A. Dolgopolov, P.R. Dudero, R. Egeland, G. Franzoni, J. Haupt, A. Inyakin³⁷, K. Klapoetke, Y. Kubota, J. Mans, N. Mirman, D. Petyt, V. Rekovic, R. Rusack, M. Schroeder, A. Singovsky, J. Zhang

University of Mississippi, University, USA

L.M. Cremaldi, R. Godang, R. Kroeger, L. Perera, R. Rahmat, D.A. Sanders, P. Sonnek, D. Summers

University of Nebraska-Lincoln, Lincoln, USA

K. Bloom, B. Bockelman, S. Bose, J. Butt, D.R. Claes, A. Dominguez, M. Eads, J. Keller, T. Kelly, I. Kravchenko, J. Lazo-Flores, C. Lundstedt, H. Malbouisson, S. Malik, G.R. Snow

State University of New York at Buffalo, Buffalo, USA

U. Baur, I. Iashvili, A. Kharchilava, A. Kumar, K. Smith, M. Strang

Northeastern University, Boston, USA

G. Alverson, E. Barberis, O. Boeriu, G. Eulisse, G. Govi, T. McCauley, Y. Musienko³⁸, S. Muzaffar, I. Osborne, T. Paul, S. Reucroft, J. Swain, L. Taylor, L. Tuura

Northwestern University, Evanston, USA

A. Anastassov, B. Gobbi, A. Kubik, R.A. Ofierzynski, A. Pozdnyakov, M. Schmitt, S. Stoynev, M. Velasco, S. Won

University of Notre Dame, Notre Dame, USA

L. Antonelli, D. Berry, M. Hildreth, C. Jessop, D.J. Karmgard, T. Kolberg, K. Lannon, S. Lynch, N. Marinelli, D.M. Morse, R. Ruchti, J. Slaunwhite, J. Warchol, M. Wayne

The Ohio State University, Columbus, USA

B. Bylsma, L.S. Durkin, J. Gilmore³⁹, J. Gu, P. Killewald, T.Y. Ling, G. Williams

Princeton University, Princeton, USA

N. Adam, E. Berry, P. Elmer, A. Garmash, D. Gerbaudo, V. Halyo, A. Hunt, J. Jones, E. Laird, D. Marlow, T. Medvedeva, M. Mooney, J. Olsen, P. Piroué, D. Stickland, C. Tully, J.S. Werner, T. Wildish, Z. Xie, A. Zuranski

University of Puerto Rico, Mayaguez, USA

J.G. Acosta, M. Bonnett Del Alamo, X.T. Huang, A. Lopez, H. Mendez, S. Oliveros, J.E. Ramirez Vargas, N. Santacruz, A. Zatzerklyany

Purdue University, West Lafayette, USA

E. Alagoz, E. Antillon, V.E. Barnes, G. Bolla, D. Bortoletto, A. Everett, A.F. Garfinkel, Z. Gecse, L. Gutay, N. Ippolito, M. Jones, O. Koybasi, A.T. Laasanen, N. Leonardo, C. Liu, V. Maroussov, P. Merkel, D.H. Miller, N. Neumeister, A. Sedov, I. Shipsey, H.D. Yoo, Y. Zheng

Purdue University Calumet, Hammond, USA

P. Jindal, N. Parashar

Rice University, Houston, USA

V. Cuplov, K.M. Ecklund, F.J.M. Geurts, J.H. Liu, D. Maronde, M. Matveev, B.P. Padley, R. Redjimi, J. Roberts, L. Sabbatini, A. Tumanov

University of Rochester, Rochester, USA

B. Betchart, A. Bodek, H. Budd, Y.S. Chung, P. de Barbaro, R. Demina, H. Flacher, Y. Gotra, A. Harel, S. Korjenevski, D.C. Miner, D. Orbaker, G. Petrillo, D. Vishnevskiy, M. Zielinski

The Rockefeller University, New York, USA

A. Bhatti, L. Demortier, K. Goulianatos, K. Hatakeyama, G. Lungu, C. Mesropian, M. Yan

Rutgers, the State University of New Jersey, Piscataway, USA

O. Atramentov, E. Bartz, Y. Gershtain, E. Halkiadakis, D. Hits, A. Lath, K. Rose, S. Schnetzer, S. Somalwar, R. Stone, S. Thomas, T.L. Watts

University of Tennessee, Knoxville, USA

G. Cerizza, M. Hollingsworth, S. Spanier, Z.C. Yang, A. York

Texas A&M University, College Station, USA

J. Asaadi, A. Aurisano, R. Eusebi, A. Golyash, A. Gurrola, T. Kamon, C.N. Nguyen, J. Pivarski, A. Safonov, S. Sengupta, D. Toback, M. Weinberger

Texas Tech University, Lubbock, USA

N. Akchurin, L. Berntzon, K. Gumus, C. Jeong, H. Kim, S.W. Lee, S. Popescu, Y. Roh, A. Sill, I. Volobouev, E. Washington, R. Wigmans, E. Yazgan

Vanderbilt University, Nashville, USA

D. Engh, C. Florez, W. Johns, S. Pathak, P. Sheldon

University of Virginia, Charlottesville, USA

D. Andelin, M.W. Arenton, M. Balazs, S. Boutle, M. Buehler, S. Conetti, B. Cox, R. Hirosky, A. Ledovskoy, C. Neu, D. Phillips II, M. Ronquest, R. Yohay

Wayne State University, Detroit, USA

S. Gollapinni, K. Gunthoti, R. Harr, P.E. Karchin, M. Mattson, A. Sakharov

University of Wisconsin, Madison, USA

M. Anderson, M. Bachtis, J.N. Bellinger, D. Carlsmith, I. Crotty¹, S. Dasu, S. Dutta, J. Efron, F. Feyzi, K. Flood, L. Gray, K.S. Grogg, M. Grothe, R. Hall-Wilton¹, M. Jaworski, P. Klabbers, J. Klukas, A. Lanaro, C. Lazaridis, J. Leonard, R. Loveless, M. Magrans de Abril, A. Mohapatra, G. Ott, G. Polese, D. Reeder, A. Savin, W.H. Smith, A. Sourkov⁴⁰, J. Swanson, M. Weinberg, D. Wenman, M. Wensveen, A. White

†: Deceased

- 1: Also at CERN, European Organization for Nuclear Research, Geneva, Switzerland
- 2: Also at Universidade Federal do ABC, Santo Andre, Brazil
- 3: Also at Soltan Institute for Nuclear Studies, Warsaw, Poland
- 4: Also at Université de Haute-Alsace, Mulhouse, France
- 5: Also at Centre de Calcul de l'Institut National de Physique Nucleaire et de Physique des Particules (IN2P3), Villeurbanne, France
- 6: Also at Moscow State University, Moscow, Russia
- 7: Also at Institute of Nuclear Research ATOMKI, Debrecen, Hungary
- 8: Also at University of California, San Diego, La Jolla, USA
- 9: Also at Tata Institute of Fundamental Research - HECR, Mumbai, India
- 10: Also at University of Visva-Bharati, Santiniketan, India
- 11: Also at Facolta' Ingegneria Universita' di Roma "La Sapienza", Roma, Italy
- 12: Also at Università della Basilicata, Potenza, Italy
- 13: Also at Laboratori Nazionali di Legnaro dell' INFN, Legnaro, Italy
- 14: Also at Università di Trento, Trento, Italy
- 15: Also at ENEA - Casaccia Research Center, S. Maria di Galeria, Italy
- 16: Also at Warsaw University of Technology, Institute of Electronic Systems, Warsaw, Poland
- 17: Also at California Institute of Technology, Pasadena, USA
- 18: Also at Faculty of Physics of University of Belgrade, Belgrade, Serbia
- 19: Also at Laboratoire Leprince-Ringuet, Ecole Polytechnique, IN2P3-CNRS, Palaiseau, France
- 20: Also at Alstom Contracting, Geneve, Switzerland
- 21: Also at Scuola Normale e Sezione dell' INFN, Pisa, Italy
- 22: Also at University of Athens, Athens, Greece
- 23: Also at The University of Kansas, Lawrence, USA
- 24: Also at Institute for Theoretical and Experimental Physics, Moscow, Russia
- 25: Also at Paul Scherrer Institut, Villigen, Switzerland
- 26: Also at Vinca Institute of Nuclear Sciences, Belgrade, Serbia
- 27: Also at University of Wisconsin, Madison, USA
- 28: Also at Mersin University, Mersin, Turkey
- 29: Also at Izmir Institute of Technology, Izmir, Turkey
- 30: Also at Kafkas University, Kars, Turkey
- 31: Also at Suleyman Demirel University, Isparta, Turkey
- 32: Also at Ege University, Izmir, Turkey
- 33: Also at Rutherford Appleton Laboratory, Didcot, United Kingdom
- 34: Also at INFN Sezione di Perugia; Universita di Perugia, Perugia, Italy
- 35: Also at KFKI Research Institute for Particle and Nuclear Physics, Budapest, Hungary
- 36: Also at Istanbul Technical University, Istanbul, Turkey
- 37: Also at University of Minnesota, Minneapolis, USA
- 38: Also at Institute for Nuclear Research, Moscow, Russia

39: Also at Texas A&M University, College Station, USA

40: Also at State Research Center of Russian Federation, Institute for High Energy Physics, Protvino, Russia